THE REPUBLIC OF TURKEY
BAHÇEŞEHİR UNIVERSITY

ADAPTIVE MODULATION WITH CHANNEL ESTIMATION IN SINGLE ANTENNA AND MULTIPLE ANTENNA SYSTEMS

Master's Thesis

MUSTAFA AL-NAQEEB

İSTANBUL, 2012

THE REPUBLIC OF TURKEY
BAHÇEŞEHİR ÜNİVERSİTESİ

THE GRADUATE SCHOOL OF NATURAL AND APPLIED SCIENCES
ELECTRICAL AND ELECTRONICS ENGINEERING

ADAPTIVE MODULATION WITH CHANNEL ESTIMATION IN SINGLE ANTENNA AND MULTIPLE ANTENNA SYSTEMS

Master's Thesis

MUSTAFA AL-NAQEEB

Supervisor: Asst. Prof. Dr. ALKAN SOYSAL

İSTANBUL, 2012

THE REPUBLIC OF TURKEY
BAHÇEŞEHİR ÜNİVERSİTESİ

THE GRADUATE SCHOOL OF NATURAL AND APPLIED SCIENCES
ELECTRICAL AND ELECTRONICS ENGINEERING

Title of Thesis: Adaptive Modulation with Channel Estimation in Single Antenna and Multiple Antenna Systems
Name of the Student: Mustafa AL-NAQEEB
Date of Thesis Defense: April 26, 2012

The thesis has been approved by the Graduate School of Natural and Applied Sciences.

Assoc. Prof. Dr. Tunç BOZBURA
Director
____

This is to certify that we have read this thesis and that we find it fully adequate in scope, quality and content, as a thesis for the degree of Master of Science.

Assoc. Prof. Dr. Ufuk TÜRELİ
Program Coordinator
____

Examining Committee Members:	Signature
Asst. Prof. Dr. ALKAN SOYSAL	___________________
Asst. Prof. Dr. Çağrı GÜNGÖR	___________________
Assoc. Prof. Dr. Ufuk TÜRELİ	___________________

ACKNOWLEDGEMENTS

First and foremost, I would like to thank my advisor, Professor Alkan Soysal for giving me the opportunity to work with him, special thanks to him for his time, patience and understanding. This thesis would not have been possible without his knowledge, supporting and motivation.

I am also indebted to the committee members of my thesis defense, Professor Çağrı Güngör and Professor Ufuk Tureli for their time and valuable comments.

I would like to thank AL-KHANJAR Organization for Scientific Development, for their financial supporting of my scholarship in Turkey, special thanks to the board director Sheikh KHAMIS AL-KANJAR and the Executive director Mr. MUSTAFA AL-KUBAISI. I cannot find words to express my gratitude to be one of their students.

In addition, I am indebted to my colleagues and research assistances in Bahçeşehir University who supported me since I started my master program, special thanks to Ömer Tura, Erinç Topdemir, Mehmet Bay and Mustafa Kılıç for their helping me and letting me using their labs to work in it.

Also, I would like to thanks my friends in Turkey and outside Turkey for their supporting me. Special thanks to my friends who came from Iraq with me, during my study period we lived together as one family, they were supporting me and encourage me to complete my studying in successful way.

Last but not least, I want to thank my beloved family, they helped and supported me during my study even that I was far away from them, without their patience, encouragement, supporting and advising me, I couldn't take any step forward. I love them so much and owe to them my deepest gratitude, and whatever I say, I will not give them their right.

Istanbul, April 2012 Mustafa Al-Naqeeb

ABSTRACT

ADAPTIVE MODULATION WITH CHANNEL ESTIMATION IN SINGLE ANTENNA AND MULTIPLE ANTENNA SYSTEMS

Mustafa Al-Naqeeb

Electrical and Electronics Engineering

Thesis Advisor: Asst. Prof. Dr. ALKAN SOYSAL

April 2012, 74 pages

The demand for high speed wireless communication systems with high quality of service (QoS) is rapidly growing. Adaptive modulation has the advantage of increasing the spectral efficiency of the communication transmission systems while keeping the quality of transmission. Adaptive modulation generally can be used by varying signal power, constellation size and coding in response to the instantaneous fade value. This thesis examines adaptive modulation schemes in single antenna and multiple antenna systems. In a single antenna system, variable rate variable power adaptive modulation with channel estimation error effects has been proposed. We derived constellation size equation which depends on the estimated channel. Two power allocation schemes have been used, water-filling and Karush–Kuhn–Tucker (KKT) based schemes. We found that data rate of the system increased with variable power schemes by at least 20 percent more than constant power allocation especially in low signal to noise ratio (SNR) values while Bit Error Rate (BER) is maintained lower than the target BER. In multiple antennas case, adaptive modulation with channel estimation error effect is studied. Variable rate constant power modulation with successive decoding technique has been implemented. We estimate the channel matrix elements separately and deal with each antenna as a single antenna system. We derive constellation size equations for each antenna and use them separately in transmitting the signal.

Keywords: Adaptive modulation, Channel estimation, MIMO, Successive decoding

ÖZET

TEK VE ÇOKLU ANTENLI SISTEMLERDE KANAL KESTIRIMI ALTINDA UYARLANABILIR MODÜLASYON

Mustafa AL-NAQEEB

Elektrik-Elektronik Mühendisliği

Tez Danışmanı: Yrd. Doç. Dr. Alkan SOYSAL

Nisan 2012, 74 sayfa

Servis kalitesi yüksek olan hızlı kablosuz haberleşme sistemlerine olan talep hızla artmaktadır. Adaptif modulasyon tekniği, iletim kalitesinden ödün vermeksizin izgesel verimliliği arttırmaktadır. Bu tez çalışmasında, tekli ve çoklu anten sistemleri için kanal kestirimi ile adaptif modülasyon yöntemleri önerilmiştir. Tekli anten sistemlerinde, kanal kestirimindeki hata etkisi göz önünde bulundurularak, değişken aktarım hızı değişken güç adaptif modulasyonu önerilmiştir. Kanal kestirimine bağlı olarak, kümelenme büyüklüğü eşitliği çıkarılmıştır. Bu eşitlikler elde edilirken, Water-filling ve Karush-Kuhn-Tucker (KKT) güç tahsis yöntemleri kullanılmıştır. Düşük sinyal gürültü oranı (SNR) için, önerilen yöntemle veri aktarım hızı, sabit güç tahsisi ile elde edilen veri aktarım hızından %20 daha yüksektir. Bit hata oranı (BER) ise, hedeflenen BER değerinden daha düşük olarak elde edilmektedir. Çoklu anten sistemlerinde, kanal kestirimindeki hata etkisi göz önünde bulundurularak, adaptif modulasyon incelenmiştir. Ardışık kod çözme tekniği kullanılarak, değişken aktarım hızı sabit güç modulasyonu önerilmiştir. Çoklu anten sistemindeki her anten, bir tekli anten sistemi olarak düşünülmüştür; böylece kanal matris elemanları ayrı ayrı kestirilmiştir. Her bir anten için kümelenme büyüklüğü eşitlikleri çıkarılmıştır. Bu eşitlikler, işaret iletiminde ayrı ayrı kullanılmıştır.

Anahtar Kelime: Adaptif modulasyon, Kanal kestirimine, MIMO, Ardışık kod çözme

CONTENTS

TABLES

FIGURES

ABBREVIATIONS

AM	:	Adaptive Modulation
AWGN	:	Additive white Gaussian noise
BER	:	Bit Error Rate
CDMA	:	Code Division Multiple Access
CIR	:	Channel Impulse Response
CSI		Channel State Information
GSM	:	Global System for Mobile Communications
ISI	:	Intersymbol interference
ISI	:	Inter Symbol Interference
KKT	:	Karush-Kuhn-Tucker Condition
LOS	:	Line of sight
LS		Least Square
MIMO	:	Multiple Input Multiple Output
MMSE	:	Minimum Mean square Error
MSE	:	Mean square error
OFDM	:	Orthogonal Frequency Division Multeplexing
PAM	:	Pulse Amplitude Modulation
PDF	:	Power density function
QAM	:	Quadrature Amplitude Modulation
QoS		Quality of Service
RF	:	Radio Frequency
SISO	:	Single input Single Output
SNR	:	Signal to Noise ratio
TDMA	:	Time Division Multiple Access
WF	:	Water Filling

SYMBOLS

Channel element	:	h_{ij}
Channel matrix	:	H
Coherence bandwidth	:	f_c
Coherence time	:	T
Constellation size	:	M
Data phase period	:	T_d
Data power	:	P_d
Data rate	:	R
Delay Spread	:	τ_{max}
Doppler spread	:	f_d
Error Probability	:	P_e
Estimated value	:	$\hat{a}$
Estimation error	:	$\tilde{a}$
Euclidean distance		d
Input signal	:	x
Input signal vector	:	X
Number of the receive Antennas	:	N_r
Number of the transmit Antennas	:	N_t
Output signal	:	y
Output signal vector	:	Y
Signal Amplitude		A_i
Signal's energy		E_s
Symbol time duration		T_s
Total power of the system	:	P
Training phase period	:	T_t
Training power	:	P_t
Variance	:	σ^2

1. INTRODUCTION

The origin of radio goes back over hundred years ago to the radio telegraphy invention by Marconi. Since Marconi's invention, wireless communication systems are improved to provide mobile, fully integrated and low cost systems that have the capability of providing high quality of voice and data transmission.

However, transmission over wireless channel can face many obstacles and limitations like multipath fading and propagation loss. With multipath fading, the transmitted signal arrives at the receiver in multiple reflective paths with different delays. These effects of multipath fading can cause fluctuations in the received signal-to-noise ratio (SNR) which increase the bit error rate (BER).

There are several techniques to decrease the effects of multipath fading channel. These techniques can be classified into non-adaptive and adaptive techniques. Non-adaptive techniques like interleaving and channel coding can be used to get an acceptable performance. Unfortunately, there is unnecessary wastage of the channel capacity because these techniques are designed for worst case channel conditions.

Adaptive techniques are a promising solution to exploit the full capacity potential of the wireless fading channel. Instead of fighting fading, the transmitter can adjust its parameters according to the channel condition when channel state information (CSI) is available at the transmitter side. This can maintain a constant performance and utilize the channel more efficiently.

1.1 LITERATURE REVIEW

Although adaptive modulation was first considered in the late 1960s, recently there has been considerable interest in improving adaptive modulation schemes. The increased demand for high data rates in wireless communications makes it a rich area for scientific research and development.

Adaptive modulation is one such scheme proposed by (Torrence & Hanzo 1996) that meets the requirements of the increased demand. There are many adaptive modulation schemes. They are different from each other by the adaptive parameters they use. In (HAYES 1968), adaptive modulation was done by changing the transmitted power to minimize the average probability of error. Also in (Narendran et al. 1997), the performance of a wireless system with power control is studied. Another type of adaptive modulation can be done by changing symbol transmission rate (Caver 1972). Adaptive rate control eliminates the effects of fading by saving 10-50dB in energy-to-noise ratio per bit from non-adaptive system for typical values of error probability. In addition, other works focus on changing constellation size (Webb & Steele 1995) (J.Torrance & Hanzo 1996) , coding rate (Vucetic 1991) (Lau & Macleod 1997) or any combination of the previous parameters (Goldsmith & Chua 1997) (Ue, Sampei & Morinaga 1996) (Goldsmith 1998) based on the instantaneous fade value. Without sacrificing BER, the main goal of all adaptive modulation schemes is to increase the data rate of transmission system.

Adaptive modulation is sensitive to the use of CSI at the transmitter. Channel can be estimated at the receiver and sent to the transmitter via a feedback link. In practice, there is no perfect channel estimation and the availability of perfect channel knowledge at the transmitter is practical when channel fading is slow relative to the data rate. Otherwise, there are delays and errors result from feedback, estimation or both. These cause a serious degradation in the performance of adaptive modulation system which are designed assuming perfect CSI (Goldsmith & Chua 1997).

Consequently, there are some works that take into account channel estimation error (Soysal, Ulukus & Clancy 2008) (Goeckel 1999) and others that use long range channel prediction methods (Alexandra, S. & H 2000) in designing adaptive transmission systems to ensure robustness of the system. In addition to previous techniques, multiple antennas are used to improve the spectral efficiency in wireless communication systems. Information theoretic results indicate that use of multiple antennas at the transmitter and receiver can meet the demand for improved performance (Telatar 1999) (Bourles & Gamal 2004). Optimizing Multiple Input Multiple Output (MIMO) resource allocations with perfect and partial CSI was considered in many works (Soysal & Ulukus 2010).

Adaptive modulation techniques have been used in different communications systems such as TDMA, CDMA, OFDM,.. etc. In a Time Division Multiple Access (TDMA) system, adaptive modulation is used to change modulation order, transmitting power, symbol rate and coding rate (MIZUNO et al. 1998) according to the condition of the channel to maximize the data rate of the transmission system. In Orthogonal Frequency Division Multiplexing (OFDM) systems adaptive modulation has been widely studied. One example is bit loading where bits are allocated to the subcarriers (Czylwik 1996) (Torabi & Soleymani 2003). The subcarrier which face a good channel has more bits and deep faded subcarriers are not used which leads to increasing in the QoS. In addition to bit loading in OFDM systems adaptive modulation is used in adapting cyclic prefix/guard time according to channel delay spread. Furthermore, adaptive modulation has also been used in Code Division Multiple Access (CDMA) systems. Adaptive modulation in CDMA is applied by changing the direct sequence or spread spectrum parameters.

Some other research considers using adaptive modulation in multiple antenna systems which leads to an increase in the data rate compared to single antenna systems (Zhendong Zhou, Dohler & Li 2005) (Fern´andez-Plazaola et al. 2010).

However, in multiple antenna systems subchannel interference is added to the total interference in the system. Several techniques are used to decrease the effect of this interference (Li & Collins 2007) (Varanasi & Guess 1997). Successive decoding is used to eliminate the effect of subchannels interference specially in multiple access systems.

1.2 CONTRIBUTIONS of THE THESIS

The main contributions of this thesis are:

a. Adaptive modulation with channel estimation in single antenna systems is studied. Two power allocation schemes are proposed. First scheme is based on Karush-Kuhn-Tucker (KKT) condition, where local optimum power allocation policy is derived by applying Lagrange multiplier to the data rate equation while keeping the power allocation constraint. The second power allocation scheme is based on Water Filling (WF) idea, which is the optimum power allocation when perfect channel knowledge is available at the receiver. We noticed increase in data rate of the system specially in low signal to noise ratio (SNR) values, while Bit Error Rate (BER) kept under the target BER.

b. Adaptive modulation with channel estimation is applied to MIMO systems. Two antennas, at both the transmitter and receiver are used, BER expression is derived for each antenna. Constant power allocation is used during transmission to decrease the complexity. Successive decoding techniques are used to decrease the interference from the first antenna in the second antenna.

1.3 THESIS OUTLINE

In this section, we give simple outline for readers to be able to keep track of this thesis.

In the second chapter, background of techniques which are used in this thesis is given.

In the third chapter, adaptive rate and power schemes in single antenna systems are studied. Two power allocation schemes are proposed to increase the data rate of system.

In the fourth chapter, adaptive modulation in 2×2 MIMO systems is considered. Successive decoding method is used in deriving BER expressions.

Finally, chapter five contains conclusions and future work.

2. OVERVIEW

In this chapter, some characteristics of digital communication systems will be explained. Figure 2.1 shows the block diagram of a single user communication system. Basically, a communication system consists of three blocks: transmitter, channel, and receiver. The main goal is to transmit and receive the signal with less number of errors. In the transmitter side, message is generated from signal source. Then, extra bits are added to the message to make the transmission of data more robust to channel effects. In the interleaver, bit stream is arranged in different temporal order before modulation process to increase its performance. Interleaving is widely used in digital communication techniques (Sadjadpour et al. 2001). Next, the binary sequence at the output of interleaver is passed to the modulator, which acts as the interface to the communication channel. The main function of the modulator is to convert the binary sequence into a waveform.

Figure 2.1: Block diagram of a single user communication system utilizing channel estimation and detection

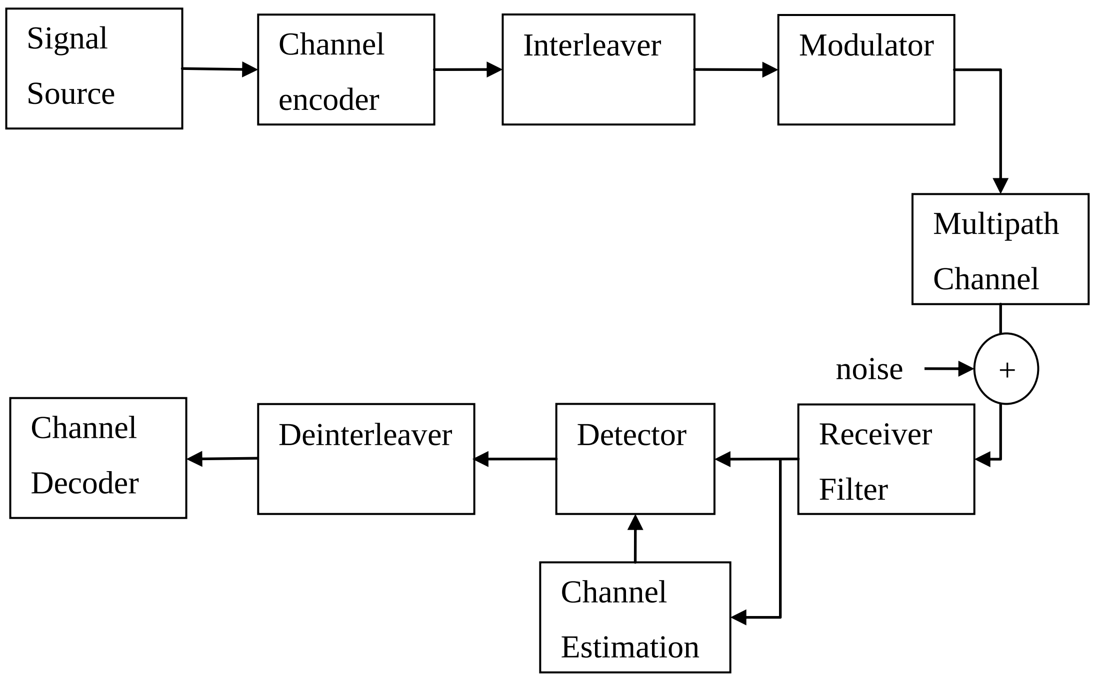

After the modulator, message is ready to be transmitted over the channel. In the channel, the transmitted signal is corrupted by multipath channel. In addition to multipath channel, noise is added to the received signal. At receiver side, the process is reversed to extract the transmitted message. First, the channel is estimated by using some channel estimation techniques. In the detector, with the presence of the estimated channel, the waveform signal is demodulated. The resulting digital bit stream from the detector is passed into the deinterleaver. Deinterleaver returns the original arrangement of the transmitted signal. Finally, channel decoder removes the extra bits to get the exact message.

2.1 WIRELESS CHANNEL

A channel can be defined as the transmission medium or electromagnetic path connects the transmitter and receiver (Proakis 2000). In a wireless communication system, the channel places an essential limitation on the quality of the transmission because the characteristics of the radio signal, which arrives at the receiver in a communication system, are not stationary and not predictable. There are many reasons for signal variations such as the physical environment of a propagation path (building, mountains, and terrain) and traveling distance (Rappaport 2002). Figure 2.2 shows the probable effects to the transmitted signal.

2.2 FADING CHANNEL MODEL

In wireless transmission systems, the transmitted signal can be corrupted by three obstructions, namely *path loss*, *shadowing*, and *multipath fading* that are considered as the transmission loss. Figure 2.3 shows the effects of path loss, shadowing, and multipath to the transmitted signal.

Figure 2.2: Wireless channel

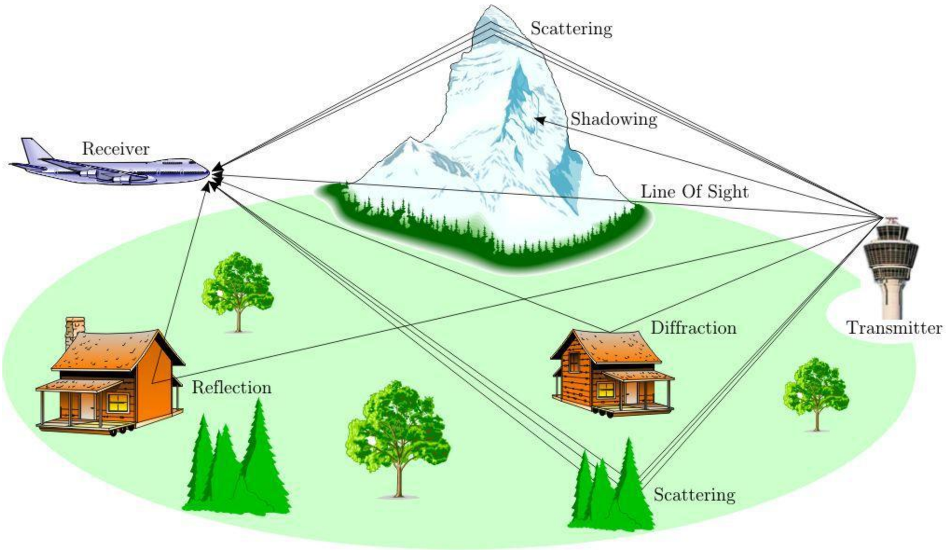

Source: Haas 2004.

2.2.1 Large Scale Fading

Large-scale fading effects consist of path loss and shadowing. Path loss results from the dissipation of power radiated by the transmitter as well as the effects of the propagation channel. While shadowing is caused by obstacles between the transmitter and receiver that attenuate signal power through absorption, reflection, and diffraction. The effect of path loss occurs over very large distances (100-1000 meters), where the effect of shadowing occurs over distances proportional to the length of the obstruction objects (Goldsmith 2005). The average path loss is expressed as a function of distance,

$$\overline{PL}(d) = \overline{PL}(d_0)\left(\frac{d}{d_o}\right)^n \qquad \textbf{(2.1)}$$

and by taking the logarithm of both sides of (2.1), the average path loss in dB becomes,

$$\overline{PL}(dB) = \overline{PL}(d_0) + 10n\log\left(\frac{d}{d_0}\right) \quad \textbf{(2.2)}$$

Since variation in received power due to path loss and shadowing occur over relatively large distances, these variations are referred to as large-scale fading. The shadowing is sometimes called lognormal fading because it has an approximate log-normal distribution.

Figure 2.3: Path Loss, Shadowing and Multipath versus Distance.

$$\textit{Transmission Loss} = \textit{Pathloss} + \textit{Shadowing} + \textit{Multipath} \quad (dB)$$

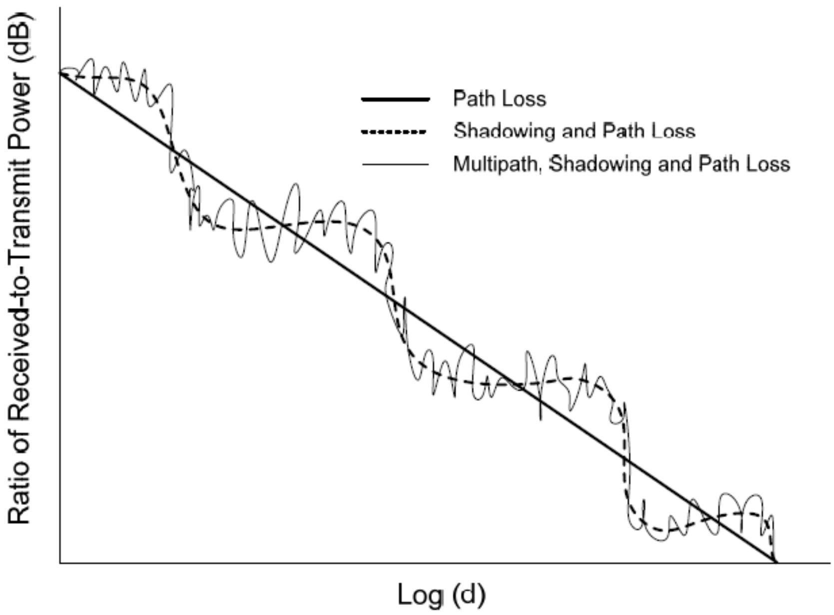

Source: Goldsmith 2005

2.3 SMALL SCALE FADING

This rapid fluctuation of the amplitudes, phases, or multipath delays of a radio signal over a period of time or travel distances is called *Fading* (Rappaport 2002). In small scale fading, the received power variation results from the constructive and destructive effects of multipath signal components. These effects that give rise to fast changes of received signal, are described by a Rayleigh distribution function, if there is no Line of

Sight (LOS) component and the number of multipath is large. Small-scale fading refers to variations that occur in the transmitted signal over short distances.

Types of small scale fading are determined by the relation between signal parameters (Bandwidth, symbol period, etc.) and the channel parameters (e.g. Doppler spread). Fading can be classified based on multipath time delay spread or Doppler spread, as illustrated in Figure 2.4

Figure 2.4: Types of Small Scale Fading

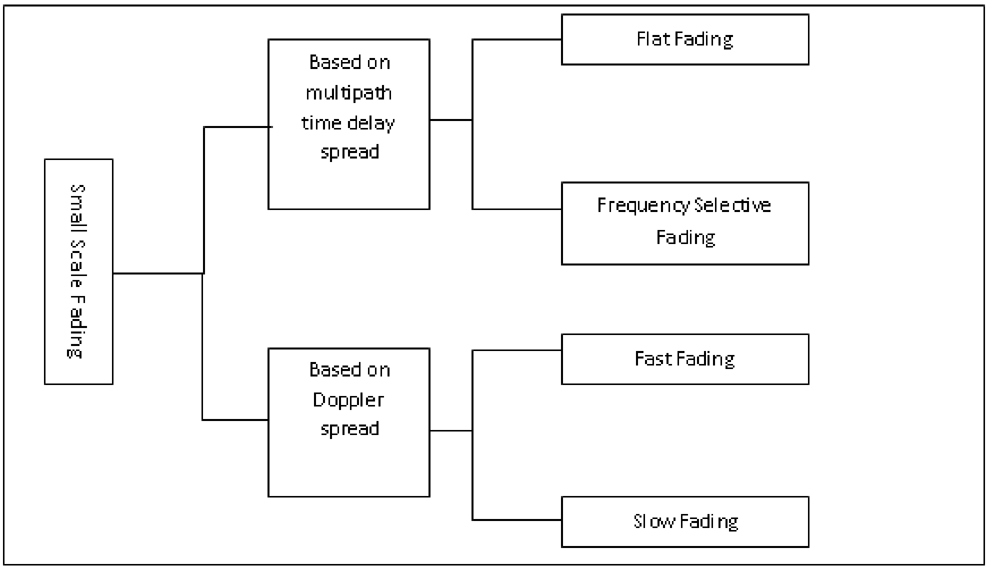

If a single pulse is transmitted over a multipath channel, the received signal will appear as multiple pulses each corresponding to a different path. In multipath channel, time delay spread may cause significant distortion in the received signal where the maximum delay spread (τ_{max}) can be defined as the time delay between the arrival of the first received signal component and the last one associated with a single transmitted pulse.

Delay spread determines how much the signal is distorted. When the delay spread is small compared to the inverse of the signal bandwidth, then there is only negligible time spreading in the received signal. However, if the delay spread is large compared to the inverse of the signal bandwidth, then this can lead to high signal distortion (Goldsmith 2005). A multipath channel can be modeled as a tap-delay line, each tap coefficient is a complex random process as the following equation:

$$h(\tau, t) = \sum_{l=1}^{L-1} \alpha_l \delta(\tau - \tau_l) \tag{2.3}$$

where L is the number of taps, α_l is the complex path gain, and τ_l is the path delay. When the bandwidth of the signal is smaller than the bandwidth of the channel then we call it *Flat Fading*. In this case the transmitted signal often arrives at the receiver within a small fraction of the symbol duration and with no change in its spectral characteristics. However, the changes appear on the amplitude of the received signal with time due to fluctuations in the gain of the channel caused by multiple paths. The coherence bandwidth is related to the maximum delay spread τ_{max} by

$$f_c = \frac{1}{\tau_{max}} \tag{2.4}$$

When the signal bandwidth is larger than the coherence bandwidth of the channel the signal faces *frequency selective fading*. In this case amplitude and phase distortion to the message are introduced by the channel, also the spectrum of the channel varies over the signal bandwidth.

Regarding to Doppler spread, multipath fading can be classified into *slow fading* and *fast fading*. The distinction between them is important for the mathematical modeling of fading channels and for the performance evaluation of communication systems operating over these channels. Coherence time T_c of the channel measures the period over which the fading process is correlated (Simon & Alouini 2005). The coherence time is related to *Doppler spread* f_d by

$$T_c = \frac{1}{f_d} \tag{2.5}$$

When the symbol time duration T_s is smaller than the channel's coefficient time T_c the fading is said to be slow; otherwise it is considered to be fast. In slow fading, a particular fade level will affect many successive symbols, which leads to burst errors, whereas in fast fading the fading does not correlate from symbol to symbol.

2.4 ADDITIVE WHITE GAUSSIAN NOISE CHANNEL MODEL

Noise can be defined as the unwanted fluctuations that are added to the received signal. In communication systems, the most general form of noise is Additive White Gaussian Noise (AWGN). the term *white* refers to the noise which has a power spectral density (PDF) independent of the operating frequency (Haykin 1994). AWGN channel has mean zero and unit variance. AWGN channel does not account for fading, frequency selectivity, interference. However, it produces simple and tractable mathematical models which are useful for gaining insight into the underlying behavior of a system before these other phenomena are considered. AWGN results from many natural sources, such as the thermal vibrations of atoms in conductors, shot noise, black body radiation from the earth and other warm objects, and from celestial sources such as the Sun (Proakis 2000, pp. 15-18).

2.5 MODULATION

Modulation is the process of converting the information from a message source into a waveform that is suitable for transmitting over the channel. In a simple way, modulation is done by translating the baseband signal to a modulated signal at a higher frequency (carrier frequency) as it is shown in Figure 2.5. Modulation can be classified into: *Analogue Modulation* and *Digital Modulation*. Analogue modulation uses Amplitude modulation and Frequency Modulation. While in digital modulation, an analogue carrier signal is modulated by a discrete signal. In modern mobile communication systems, digital modulation techniques are commonly used, since it offers many advantageous such as: high data rate, powerful error correction techniques, more flexibility and greater robustness to channel impairments (Goldsmith 2005). There are several types of digital modulation forms. In this thesis, Pulse Amplitude Modulation (PAM) and Quadrature Amplitude Modulation (QAM) are considered.

Figure 2.5: Modulation

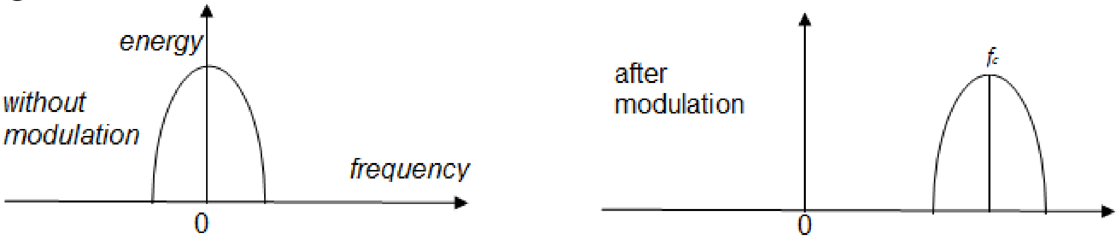

2.5.1 Pulse Amplitude Modulation (PAM)

PAM is considered as the simplest form of linear modulation, it does not have a quadratue component and it is considered as one dimensional modulation. In M-ary PAM, all the information is encoded into the signal amplitude A_i. Mathematically, the transmitted signal over one symbol time is given by

$$s_i(t) = \Re\{A_i g(t) e^{j2\pi f_c t} = A_i g(t)\cos(2\pi f_c t) \quad 0 \le t \le T_S \gg \frac{1}{f_c} \qquad \textbf{(2.6)}$$

where $\{ A_i, 1 \le i \le M\}$ denote the set of M possible amplitudes and $M = 2^k$ possible k-bit blocks of symbols. The signal amplitudes A_i take the following discrete values (Proakis 2000)

$$A_i = (2i - 1 - M)d \quad ,i = 1,2, \ldots., M \qquad \textbf{(2.7)}$$

where $2d$ is the distance between adjacent signal amplitudes.
The MPAM signals have the energy

$$
\begin{aligned}
E_{s_i} &= \int_0^{T_s} s_i^2(t)dt \\
&= \int_0^{T_s} A_i^2 g^2(t)\cos^2(2\pi f_c t)dt = A_i^2
\end{aligned}
\tag{2.8}
$$

2.5.1.1 Constellation mapping

In MPAM, the constellation mapping is done by using Gray encoding, where the adjacent signal amplitudes differ by one binary bit as it is shown in Figure 2.6. The main reason behind choosing Gray codes in MPAM is that in the demodulation of the signal, the most likely errors result from due to the erroneous selection of an adjacent amplitude to the transmitted signal amplitude (Proakis 2000). This erroneous selection causes only a single bit error in the sequence of *k* bits, when Gray encoding is used.

Figure 2.6: MPAM constellations diagrams

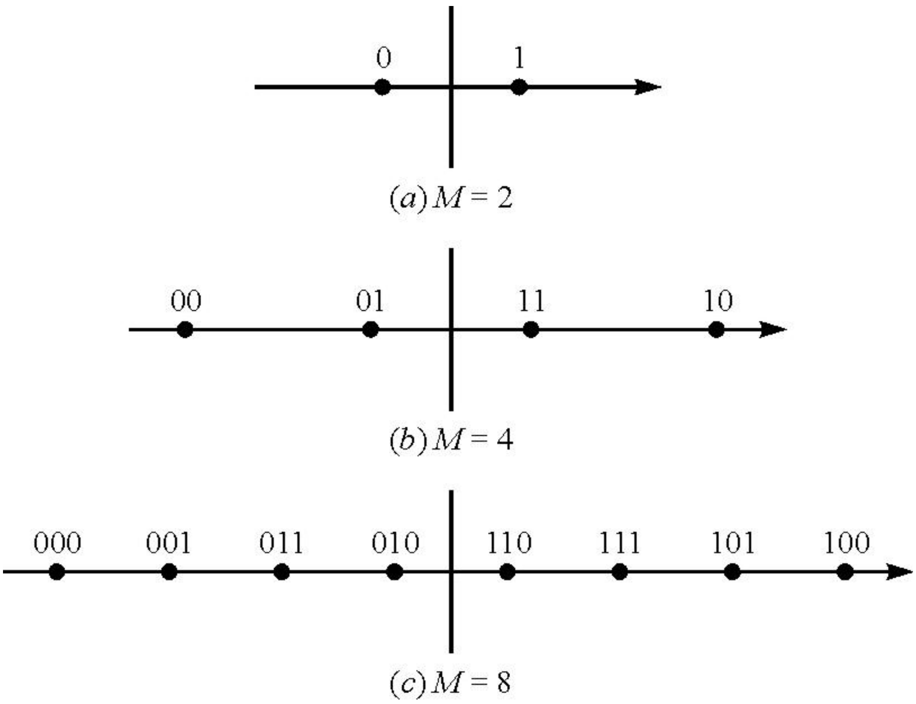

Source: Proakis 2000

2.5.2 M-ary Quadrature Amplitude Modulation (MQAM)

In MQAM, the information sequence is encoded into amplitude and phase of the transmitted signal. MQAM can encode the most number of bits per symbol for a given energy (Goldsmith 2005). The mathematical description of the signal is given as

$$
\begin{aligned}
s_i(t) &= \Re\{A_i e^{j\theta} g(t) e^{j2\pi f_c t} \\
&= A_i \cos(\theta_i)\, g(t) \cos(2\pi f_c t) - A_i \sin(\theta_i)\, g(t) \cos(2\pi f_c t) \\
&\qquad 0 \leq t \leq T_S \gg \frac{1}{f_c}
\end{aligned}
\qquad \textbf{(2.9)}
$$

MQAM is similar to MPAM except that in MQAM the signal is put in the in-phase and quadrature modulation term with 90^o phase shift between them. Figure 2.7 shows several signal space diagrams for rectangular QAM. Usually constellation size value *M* takes numbers of multiple two.

Figure 2.7: Constellation Map of MQAM

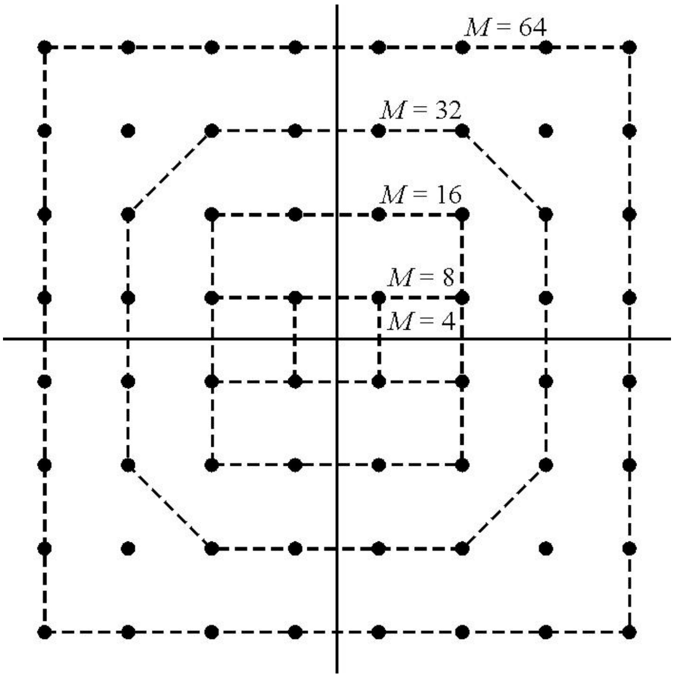

Source: (Proakis 2000)

In fact, the square MQAM can be easily implemented by combining two $\sqrt{M}$-PAM. Example of signals space diagrams for 64-QAM as a combination of two 8-PAM is shown in Figure 2.8.

Figure 2.8:(a) 64 M-QAM constellation (b) Equivalent in-phase and quadrature component 8-PAM constellations

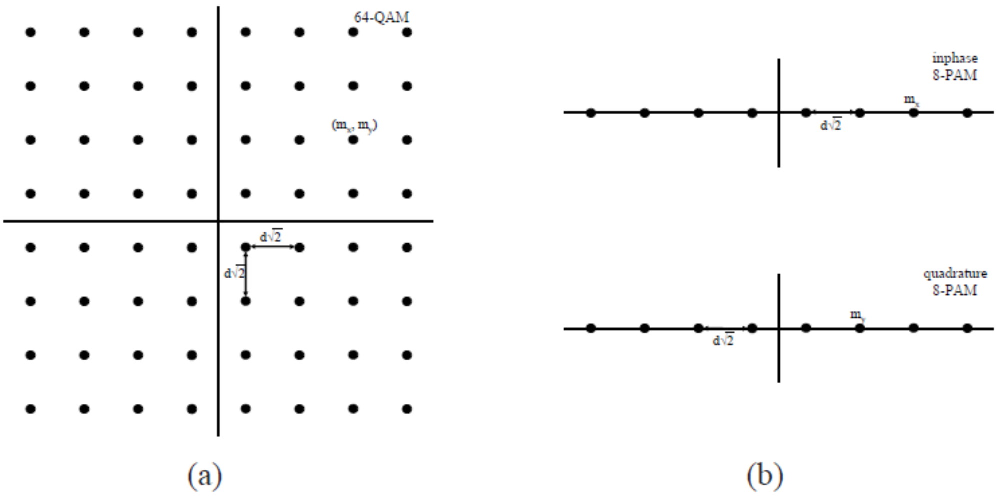

Source: Soysal, Ulukus & Clancy 2008

2.6 CHANNEL ESTIMATION

Channel estimation is a challenging problem in wireless systems. It plays a key role as the performance of the decoding process depends on how accurate the channel knowledge is. A dynamic channel estimation is required in wireless communication system before the demodulation process in the receiver side since the transmitted signal is corrupted by a fading channel and AWGN effects. Channel estimation techniques can be classified into two categories: blind and non-blind (OZDEMIR & HUSEYIN ARSLAN 2007). The blind channel estimation methods exploit the statistical behavior of the received signal and require a large amount of data. In the non-blind channel estimation, training bits that are known at the receiver are transmitted. In this thesis non-blind channel estimation in particular Minimum Mean Square Error (MMSE) technique is investigated.

Usually the channel is estimated at the receiver based on the known training sequence which is transmitted in every block as in Figure 2.9. In the receiver side, known training sequence is extracted and the channel is estimated by estimation techniques. Then, data sequence is decoded.

Figure 2.9: GSM block structure

Tail	Data	Training	Data	Tail
3	58	26	58	3

There are several channel estimation techniques in wireless communication systems. An estimation technique is considered to be good, if it results in a small error probability. In this thesis, linear MMSE channel estimator is used since it is optimum when channel is Gaussian.

2.6.1 Linear Minimum Mean Square Error (MMSE)

Linear MMSE estimator yields much better performance than the other estimators. However, the main drawback of the MMSE estimator is its high computational complexity.

Let $\boldsymbol{a}$ and $\boldsymbol{b}$ be a random vectors, an estimator $\widehat{\boldsymbol{a}} = \mathbf{M}\boldsymbol{b}$ is a function of $\boldsymbol{b}$ with mean square error (MSE)

$$MSE = E\{(\widehat{\boldsymbol{a}} - \boldsymbol{a})^2\} \qquad \textbf{(2.10)}$$

where $E\{X\}$ refers to the mean of X and $\boldsymbol{M}$ is the matrix which satisfies MMSE condition.

The estimator $\widehat{\boldsymbol{a}}$ which minimizes (2.10**)** is called MMSE estimator. Calculating the linear MMSE can be done by using orthogonality principle (Kamen & Su 1999) which states that channel estimation error is orthogonal to the observation vector ***b*.** Then the matrix **M** can be found as the following,

$$E[(\boldsymbol{\hat{a}} - \boldsymbol{a})\boldsymbol{b^H}] = 0 \quad \textbf{(2.11)}$$

$$E[\boldsymbol{\hat{a}b^H} - \boldsymbol{ab^H}] = 0 \quad \textbf{(2.12)}$$

Since $\boldsymbol{\hat{a}} = \mathbf{M}\boldsymbol{b}$ then

$$E[\mathbf{M}\boldsymbol{bb^H} - \boldsymbol{ab^H}] = 0 \quad \textbf{(2.13)}$$

Since the expectation is linear then $E[A + B] = E[A] + E[B]$ and $E[Ca] = C(E[a])$ where C is constant. This leads to

$$\mathbf{M}(E[\boldsymbol{bb^H}]) - E[\boldsymbol{ab^H}] = 0 \quad \textbf{(2.14)}$$

Then the matrix **M** which satisfies linear MMSE is

$$\mathbf{M} = E[\boldsymbol{ab^H}](E[\boldsymbol{bb^H}])^{-1} \quad \textbf{(2.15)}$$

2.7 ADAPTIVE MODULATION

Adaptive modulation techniques for wireless communications have received significant interest in the few past decades (J.Pons & J.Dunlup 1998). Adaptive algorithms have been shown to be promising and effective techniques to increase the performance of the transmission system in radio channels due to their advantages of flexibility, quality of transmission and the efficient use of the frequency spectrum which increase the capacity and the reliability in wireless communication systems. Adaptive algorithms can be implemented by changing modulation parameters (such as modulation order, power,..etc) dynamically according to the channel condition. Therefore, when the channel is good, transmitter can use a higher modulation order with more power so the data rate increases. On the other hand, when the channel is bad, a lower modulation order is used to save power for better channels. This changing in transmission parameters makes the system flexible and results in using the frequency spectrum efficiently which gives us high data rate and good transmission quality.

In non-adaptive modulation systems the transmitter does not change its parameters. Non-adaptive modulation uses fixed modulation order to get a certain data rate and to guarantee the quality of transmission at the same time. In other words, in non-adaptive modulation, system parameters (such as: constellation size, power,..) are specified before transmission, and kept constant. However, this strategy is not optimal since channel varies randomly in time. Therefore, power can be wasted in some good channels and there might be no guarantee in QoS.

2.7.1 Fixed Modulation Systems

Fixed modulation techniques carry the same number of bits over different realizations of the channel. Fixed Modulation systems have been studied and used in various ways for many different channels. Modulation order can be chosen depending on previous knowledge or special channel in mind to decrease the probability of error and increase system performance.

Signal in the wireless communication channel is corrupted at least by AWGN and interference, therefore detection of the transmitted signal is never free from making errors. The detector can be designed in various ways, depending on the availability of channel model and modulation method. There are different detection schemes used in wireless communication system, the optimum detector is supposed to find the most likely transmitted symbol given a received signal. However, it is very complex to implement. Therefore, less complex suboptimum detection schemes are used in wireless communication systems (Proakis 2000). BER is defined as the average number of the errors divided by the total number of transmitted bits. BER depends on the detector and channel. Therefore, for AWGN which only adds white Gaussian noise to the transmitted signal, BER is completely specified by the signal to noise ratio (SNR) in the detector. There are several techniques to decrease the effect of AWGN channel and increasing data rate such as increasing SNR to increase the number of the transmitted bits which provide efficiency in using bandwidth. Furthermore, moving the transmitter and receiver close together (if possible) can increase the gain in SNR too. In addition to AWGN, most of wireless channels are affected by fading. In multipath fading case large power is needed to improve the transmission system under certain average BER. For example in fading channel with fixed modulation system, the received SNR varies with time. Without adaptive modulation techniques in Rayleigh fading channel for BPSK it requires average SNR=24 dB to obtain spectral efficiency 1 at 10^{-3} BER (Goldsmith & Chua 1997), in these power and BER specifications adaptive modulation can provide more spectral efficiency.

2.7.2 Adaptive Modulation

Although adaptive modulation was first proposed in 1960s (HAYES 1968) there are many researches consider adaptive modulation systems to improve the spectral efficiency on time-varying fading channel. Instead of fighting the fading channel, the transmitter can take advantage of it by changing its parameters such as transmitted power level, constellation size, symbol transmission rate and coding scheme based on the instantaneous fade value.

In this section, we will give an overview of adaptive modulation systems and their performance with perfect channel estimation and imperfect channel estimation case.

2.7.3 Perfect Channel Estimation

In this type of adaptive modulation system, the channel gain is assumed to be perfectly known at both the receiver and the transmitter. It is also assumed that there is a feedback link from the receiver to the transmitter and it has no delay. This case of adaptive modulation systems have been well studied in (Goldsmith & Chua 1997) (Chung & Goldsmith 2001). In this section we will use the same notation in (Chung & Goldsmith 2001). Let's assume $\bar{s}, \sigma^2, B$ and $\bar{g}$ refer to average transmit power, noise variance, bandwidth and average channel power gain, respectively. When the transmitter power is constant, the instantaneous SNR is $\gamma[l] = \frac{\bar{s}g[l]}{\sigma^2}$. It is assumed that

$\gamma[l]$ has probability density function (pdf) denoted by $p(\gamma)$ which is independent of l because it is stationary and its value depends on channel type. For example, in Rayleigh fading channel, pdf is given as

$$p(\gamma) = \begin{cases} \frac{1}{\Gamma}\exp\left(-\frac{\gamma}{\Gamma}\right), & \gamma \geq 0 \\ 0, & \gamma < 0 \end{cases} \tag{2.16}$$

where $\Gamma = \frac{\bar{S}}{\sigma^2}$ is equal to the average SNR in the receiver.

One of the simplest form of adaptive modulation is implemented by using variable rate system with constant power, while BER can be kept under certain maximum value. In this case, however, a cutoff value of channel power gain is specified and no transmission should be done under this value. Assuming that using N different constellations where $0 \leq i \leq N-1$, the transmit power

$$S(\gamma) = \begin{cases} S, & \gamma \geq \gamma_0 \\ 0, & \gamma < \gamma_0 \end{cases} \tag{2.17}$$

where S is given as

$$E[S(\gamma)] = S\int_{\gamma_0}^{\infty} p(\gamma)d\gamma = \bar{S} \tag{2.18}$$

Such that for all γ, the average transmitted power is used. While adaptation techniques by changing system rate is applied, BER of the system must also be taken into account. BER for modulation i at received SNR equal to $\frac{\gamma_i S}{\bar{S}}$ should be less than the designed target BER$_t$. Thus $BER_i\left(\frac{\gamma_i S}{\bar{S}}\right) \leq BER_t$ for $0 \leq i \leq N-1$.

2.7.4 Adaptive Rate and Power Systems

Here, we turn our attention to the most general case of adaptive QAM modulation systems, where both the rate and the transmitted power are chosen based on the channel condition to improve the efficiency. We will consider variable rate variable power system which has been proposed in (Goldsmith & Chua 1997). The constellation size is found by deriving BER bound for every γ as the following,

$$BER(\gamma) \leq .2 \exp\left(-\frac{1.5\gamma}{M-1}\frac{S(\gamma)}{\bar{S}}\right) \tag{2.19}$$

Then we can adjust M to keep BER constant. By rearranging (2.19) we can get the maximum constellation size for a given BER:

$$M(\gamma) \leq 1 + \frac{1.5\gamma}{-\ln(5BER)}\frac{S(\gamma)}{\bar{S}} \tag{2.20}$$

After that, spectral efficiency can be maximized by solving the following optimization problem

$$\max E[\log_2 M(\gamma)] = \int \log_2\left(1 + \frac{1.5\gamma}{-\ln(5BER)}\frac{S(\gamma)}{\bar{S}}\right)p(\gamma)d\gamma \tag{2.21}$$

Subject to the power constraint

$$\int S(\gamma)p(\gamma)d\gamma = \bar{S} \tag{2.22}$$

While adapting power is made by using water-filling power allocation techniques. Therefore, we will have

$$\frac{S(\gamma)}{\bar{S}} = \begin{cases} \frac{1}{\gamma_o} - \frac{1}{\gamma K}, & \gamma \geq \frac{\gamma_0}{K} \\ 0 \qquad\quad , & \gamma \leq \frac{\gamma_0}{K} \end{cases} \qquad \textbf{(2.23)}$$

Where $K = -\frac{1.5}{\ln(5BER)}$ and the cut off fading gain is $\frac{\gamma_0}{K}$

2.7.5 Adaptive Modulation with Channel Estimation Error

In the previous section, we explained adaptive modulation techniques by assuming that there is perfect knowledge of the channel at both the transmitter and receiver. However, channel in practical case is never estimated perfectly and there is channel estimation error. Channel estimation error can decrease the performance of the modulator. Effects of channel estimation error has been widely studied (Xia & Wang 2005) (Tang, Alouini & Goldsmith 1999). In (Soysal, Ulukus & Clancy 2008) channel estimation error is considered in designing an adaptive modulation system. BER expression is derived by using Maximum Likelihood Rule which states that the signal point (i, j) is decoded if $f(y|m_x, m_y)$ is maximum for $m_x = i, m_y = j$. In the next chapters, adaptive modulation with channel estimation error is studied with single antenna and multiple antenna systems.

3. ADAPTIVE MODULATION IN SINGLE ANTENNA SYSTEMS

In this chapter, adaptive modulation is studied in a point-to-point channel with a single antenna at both ends. The channel between the transmitter and the receiver is represented by a circularly-symmetric complex Gaussian random variable $h,$ i.e., Rayleigh fading. A block fading scenario is considered where the channel stays constant for T symbols and changes to an independent and identically distributed (i.i.d) realization during block transitions. The received signal can be represented as

$$\boldsymbol{y} = \sqrt{P}h\boldsymbol{x} + \boldsymbol{n} \tag{3.1}$$

where $\boldsymbol{n}$ is a zero-mean, unit-variance, circularly symmetric complex Gaussian noise. The input signal $\boldsymbol{x}$ has a unit average power constraint, $E[|\boldsymbol{x}|^2] \leq 1$, P is the average (SNR).

In this model each block is divided into training and data transmission phases, where the training sequence has length T_t, and the data sequence has length $T_d = T - T_t$. In order to demodulate the transmitted symbols, the channel has to be estimated at the receiver side. A setting is considered where the transmitter sends training symbols that are known at the receiver. Receiver can estimate the channel using these training symbols and feed the estimated channel back to the transmitter. Feedback is assumed to be error free and instantaneous in this analysis, since we focus on the effect of the channel estimation error.

3.1 CHANNEL ESTIMATION:

Channel estimation is an important part in adaptive modulation system since the transmitter changes its parameters due to channel condition. To assure good channel quality, known training bits to the receiver are sent from the transmitter with training power therefore receiver can estimate the channel by some channel estimation techniques (MMSE, ML,..etc). The input-output relation of the channel during the training phase is

$$\mathbf{y_t} = \sqrt{\mathrm{P_t}}\mathrm{h}\mathbf{x_t} + \mathbf{n_t} \qquad \textbf{(3.2)}$$

where P_t is the SNR of the training symbol, and length T_t vectors $\boldsymbol{y_t}$, $\boldsymbol{x_t}$ and $\boldsymbol{n_t}$ represent the received signal, the transmitted signal and the noise, respectively. The power constraint for the training input signal becomes $\frac{1}{T_t}\boldsymbol{x_t^H}\boldsymbol{x_t} \leq 1$. When the received signal y_t arrives at the receiver side, receiver will estimate the channel $\hat{h}$ which can be any function of $\boldsymbol{x_t}$ and $\boldsymbol{y_t}$, that is, $\hat{h} = f(\boldsymbol{x}_t, \boldsymbol{y}_t)$. Here, channel is estimated by linear (MMSE) estimation method, since it is optimum when the channel follows complex Gaussian distribution. We have the following optimization problem with $\hat{h} = \boldsymbol{c^H}\boldsymbol{y_t}$ and $\tilde{h} = h - \hat{h}$,

$$\min_{\boldsymbol{c}} \boldsymbol{E}\left[\widetilde{\boldsymbol{h}}\widetilde{\boldsymbol{h}}^*\right] = \min_{\boldsymbol{c}} \boldsymbol{E}[(\boldsymbol{h} - \boldsymbol{c^H}\boldsymbol{y_t})(\boldsymbol{h} - \boldsymbol{c^H}\boldsymbol{y_t})^*] \qquad \textbf{(3.3)}$$

To minimize the channel estimation error and solve the above equation, orthogonality principle between the hermitian transpose of training output $\boldsymbol{y}_t^H$ and channel estimation error $\tilde{h}$ ($E\left[\tilde{h}\boldsymbol{y}_t^H\right] = 0$) and the matrix inversion lemma are applied. Therefore, the estimated channel is found as

$$\begin{aligned} &E\left[\left(h - \hat{h}\right)\boldsymbol{y}_t^H\right] = 0 \\ &E[(h - \boldsymbol{c^H}\boldsymbol{y_t})\boldsymbol{y}_t^H] = 0 \\ &E[h\boldsymbol{y}_t^H - \boldsymbol{c^H}\boldsymbol{y_t}\boldsymbol{y}_t^H] = 0 \end{aligned} \qquad \textbf{(3.4)}$$

By using the linearity property of the expectation process and inserting (3.2) in (3.4**),** we have

$$E\left[h\left(\sqrt{\mathrm{P_t}}\mathrm{h}\mathbf{x_t}+\mathbf{n_t}\right)^{\mathrm{H}}\right]=\mathbf{c}^{\mathrm{H}}\mathrm{E}\left[\left(\sqrt{\mathrm{P_t}}\mathrm{h}\mathbf{x_t}+\mathbf{n_t}\right)\left(\sqrt{\mathrm{P_t}}\mathrm{h}\mathbf{x_t}+\mathbf{n_t}\right)^{\mathrm{H}}\right] \quad \textbf{(3.5)}$$

since h and $\boldsymbol{n_t}$ are independent to each other, then the expectation over them is zero. Therefore $\boldsymbol{c}^H$ which satisfy (3.3) is

$$\mathbf{c}^{\mathrm{H}}=\frac{\sqrt{P_t}\boldsymbol{x}_t^H}{1+P_t\boldsymbol{x}_t^H\boldsymbol{x}_t} \quad \textbf{(3.6)}$$

And the estimated channel becomes,

$$\hat{h}=\frac{\sqrt{P_t}\boldsymbol{x}_t^H\boldsymbol{y}_t}{1+P_t\boldsymbol{x}_t^H\boldsymbol{x}_t} \quad \textbf{(3.7)}$$

After estimating the channel, the channel is fed back to the transmitter and the transmitter regards the estimated channel as the actual channel while channel estimation error is added to the noise.

3.2 DATA TRANSMISSION PHASE:

In this process the received signal can be written as

$$\boldsymbol{y}_d=\sqrt{P_d(\hat{h})}(\hat{h}+\tilde{h})\boldsymbol{x}_d+\boldsymbol{n}_d \quad \textbf{(3.8)}$$

$$=\sqrt{P_d(\hat{h})}\,\hat{h}\boldsymbol{x}_d+\sqrt{P_d(\hat{h})}\,\tilde{h}\,\boldsymbol{x}_d+\boldsymbol{n}_d \quad \textbf{(3.9)}$$

Where $P_d(\hat{h})$ is the instantaneous SNR with $E\left[P_d(\hat{h})\right] = P_d$, and $\boldsymbol{x}_d$ is a complex valued input signal which is a point in M-QAM constellation. In this thesis, we assume square constellation because of its ease of implementation. Square M-QAM is considered as a combination of two $\sqrt{M}$-PAM, one in in-phase part and the other in quadrature part. The value of one dimensional signal point has value $\frac{A_i}{\sqrt{2}}$ in $\sqrt{M}$-PAM and the amplitude A_i is given by

$$A_i = \left(2i - 1 - \sqrt{M}\right)d \tag{3.10}$$

By assuming equally probable signals, the average energy of the in-phase component is

$$\begin{aligned} \frac{P_d(\hat{h})T_p}{2} &= \frac{1}{\sqrt{M}} \sum_{i=1}^{\sqrt{M}} \frac{A_i^2}{2} \\ &= \frac{(M-1)d^2}{6} \end{aligned} \tag{3.11}$$

In a M-QAM system, A_i is transmitted as the in-phase component and A_j as the quadrature component. Then, the complex received signal after match filtering can be written as

$$\boldsymbol{y} = \frac{1}{\sqrt{2}} A_{ij} h + \boldsymbol{n} \tag{3.12}$$

where $A_{ij} = A_i + jA_j$ and $h = h_x + jh_y$. As we mentioned before, there is no perfect channel estimation and channel estimation error exists. Then

$$\boldsymbol{y} = \frac{1}{\sqrt{2}} A_{ij} \hat{h} + \frac{1}{\sqrt{2}} A_{ij} \tilde{h} + \boldsymbol{n} \tag{3.13}$$

In our model, channel estimation error is added to the noise and the receiver regards the estimated channel $\hat{h}$ as the actual channel and $\frac{1}{\sqrt{2}} A_{ij} \tilde{h} + \boldsymbol{n}$ as the effective noise.

3.2.1 Decision Regions with Channel Estimation Error

In order to find the decision regions when there is channel estimation error in the transmission system, maximum likelihood rule is utilized which states that (i, j) is decoded if $f(\boldsymbol{y}|m_x, m_y)$ is maximum for $m_x = i$, $m_y = j$. Therefore, for the in-phase component the decision region can be found by satisfying

$$
\begin{aligned}
&f(\boldsymbol{y}|i, j, \hat{h}) \geq f(\boldsymbol{y}|i+1, j, \hat{h}) \\
&f(\boldsymbol{y}|i, j, \hat{h}) \geq f(\boldsymbol{y}|i-1, j, \hat{h})
\end{aligned} \tag{3.14}
$$

After assuming that pdf's always intersect with their neighbors (Soysal, Ulukus & Clancy 2008), the right side boundary of the decision region corresponding to *i* can be found by solving

$$
f(\boldsymbol{y}|i, j, \hat{h}) = f(\boldsymbol{y}|i+1, j, \hat{h})
$$

$$
\frac{\exp\left(-\frac{\left(\boldsymbol{y} - \frac{A_i}{\sqrt{2}}|\hat{h}|\right)^2}{2\tilde{\sigma}_i^{\,2}}\right)}{\sqrt{\tilde{\sigma}_i^2}} = \frac{\exp\left(-\frac{\left(\boldsymbol{y} - \frac{A_i}{\sqrt{2}}|\hat{h}| - \sqrt{2}d|\hat{h}|\right)^2}{2\tilde{\sigma}_{i+1}^{\,2}}\right)}{\sqrt{\tilde{\sigma}_{i+1}^2}} \tag{3.15}
$$

where $\tilde{\sigma}_i^2 = \frac{1}{2}\left(\frac{A_i^2+A_j^2}{2}\sigma_{\tilde{h}}^2 + 1\right)$ is the variance of the in-phase component of the effective noise and $\sigma_{\tilde{h}}^2$ is the variance of channel estimation error. By taking natural logarithm of (3.15) and assuming $\tilde{\boldsymbol{n}} = \boldsymbol{y} - \frac{A_{mx}}{\sqrt{2}}\left|\hat{h}\right|$, we have

$$\ln(\tilde{\sigma}_i^2) + \frac{\tilde{\boldsymbol{n}}^2}{\tilde{\sigma}_i^2} = \ln(\tilde{\sigma}_{i+1}^2) + \frac{\left(\tilde{\boldsymbol{n}} - \sqrt{2}d\left|\hat{h}\right|\right)}{\tilde{\sigma}_{i+1}^2} \qquad \textbf{(3.16)}$$

To simplify the calculation of $\tilde{\boldsymbol{n}}$, it is assumed that non-canceling terms containing square of $\tilde{\boldsymbol{n}}$ are small enough (Soysal, Ulukus & Clancy 2008), then

$$\begin{aligned}\tilde{\boldsymbol{n}} &= \frac{d\left|\hat{h}\right|}{\sqrt{2}} + \frac{\tilde{\sigma}_{i+1}^2}{2\sqrt{2}d\left|\hat{h}\right|}\ln\left(\frac{\tilde{\sigma}_{i+1}^2}{\tilde{\sigma}_i^2}\right) \\ &= \frac{d\left|\hat{h}\right|}{\sqrt{2}} + r_{i|j} \triangleq \bar{r}_{i|j}\end{aligned} \qquad \textbf{(3.17)}$$

where $r_{i|j}$ is the shift of the decision region on the right edge of signal point, *i*. In similar way, the left edge of the decision regions becomes,

$$\begin{aligned}\tilde{\boldsymbol{n}} &= -\left(\frac{d\left|\hat{h}\right|}{\sqrt{2}} + \frac{\tilde{\sigma}_{i-1}^2}{2\sqrt{2}d\left|\hat{h}\right|}\ln\left(\frac{\tilde{\sigma}_i^2}{\tilde{\sigma}_{i-1}^2}\right)\right) \\ &= -\left(\frac{d\left|\hat{h}\right|}{\sqrt{2}} - l_{i|j}\right) \triangleq \bar{l}_{i|j}\end{aligned} \qquad \textbf{(3.18)}$$

where $l_{i|j}$ is the shift of the decision region on the left edge of signal point, *i*. After finding $\bar{r}_{i|j}$ and $\bar{l}_{i|j}$, the decision region corresponding to i can be found by combining both edges

$$-\frac{d|\hat{h}|}{\sqrt{2}} + l_{i|j} \leq \tilde{\boldsymbol{n}} \leq \frac{d|\hat{h}|}{\sqrt{2}} + r_{i|j} \tag{3.19}$$

Now, the in-phase probability of error can be written as the following

$$\begin{aligned} P_{i|j} &= \Pr\left(-\bar{l}_{i|j} < \tilde{\boldsymbol{n}} < \bar{r}_{i|j} \middle| \hat{h}, i, j\right) \\ &= Q\left(\frac{\bar{l}_{i|j}}{\tilde{\sigma}_i}\right) + Q\left(\frac{\bar{r}_{i|j}}{\tilde{\sigma}_i}\right) \end{aligned} \tag{3.20}$$

Since the right-side boundary for i is the left-side boundary for $i + 1$, we have the following,

$$\sum_i P_{i|j} = \sum_i 2Q\left(\sqrt{\frac{\bar{r}_{i|j}^2}{\tilde{\sigma}_i^2}}\right) \tag{3.21}$$

Since Q function is decreasing function and after neglecting the square term of $\bar{r}_{i|j}$, we have

$$\sum_i P_{i|j} < \sum_i 2Q\left(\sqrt{\frac{d^2|\hat{h}|^2}{2\tilde{\sigma}_i^2} + 2\frac{d|\hat{h}|r_{i|j}}{\sqrt{2}\tilde{\sigma}_i^2}}\right) \tag{3.22}$$

By inserting $r_{i|j}$ into (3.22), we have

$$\sum_i P_{i|j} < \sum_i 2Q\left(\sqrt{\frac{d^2|\hat{h}|^2}{2\tilde{\sigma}_i^2} + \frac{\tilde{\sigma}_{i+1}^2}{2\tilde{\sigma}_i^2}\ln\left(\frac{\tilde{\sigma}_{i+1}^2}{\tilde{\sigma}_i^2}\right)}\right) \tag{3.23}$$

The upper bound of the in-phase probability of error can be found by averaging the above inequality over i. Therefore, the second term inside the Q function will be zero and the in-phase probability of error becomes

$$P_{in} \lesssim 2Q\left(\sqrt{\frac{d^2\left|\hat{h}\right|^2}{2(P_d\left(\hat{h}\right)\sigma_{\tilde{h}}^2 + 1}}\right) \tag{3.24}$$

Finally, by using the approximate value of Q-function $Q(x) \approx \frac{1}{2}\exp(-x^2)$, and inserting d, the in-phase probability of error becomes

$$P_{in} \lesssim \exp\left(-\frac{3P_d\left(\hat{h}\right)\left|\hat{h}\right|^2}{(M-1)\left(P_d\left(\hat{h}\right)\sigma_{\tilde{h}}^2 + 1\right)}\right) \tag{3.25}$$

Now BER of M-QAM over the in-phase and quadrature components becomes

$$\begin{aligned} BER(h) &\leq P_{in} + P_q \\ &\lesssim 2\exp\left(\frac{-3P_d\left(\hat{h}\right)\left|\hat{h}\right|^2}{(M-1)\left(P(h)\sigma_{\tilde{h}}^2 + 1\right)}\right) \end{aligned} \tag{3.26}$$

In order to choose the constellation size, target BER can be equated to the right hand side of (3.26), so the maximum constellation size with BER less than or equal target BER is calculated as

$$M\left(\hat{h}\right) = 1 + K\frac{P_d\left(\hat{h}\right)\hat{h}^2}{P_d\left(\hat{h}\right)\sigma_{\tilde{h}}^2 + 1} \tag{3.27}$$

where $K = -\frac{3}{\ln(.5BER)}$. Since square number of constellation size is used, the resulting $M(\hat{h})$ is approximated by the first square number less than $M(\hat{h})$. Table 3.1 shows the approximating procedure for each value of $M(\hat{h})$.

Table 3.1: Corresponding value of M for each $\mathbf{M(\hat{h})}$

$M(\hat{h})$	M
$0 \leq M(\hat{h}) < 2$	0
$2 \leq M(\hat{h}) < 4$	2
$4 \leq M(\hat{h}) < 16$	4
$16 \leq M(\hat{h}) < 64$	16
$64 \leq M(\hat{h}) < 256$	64
$256 \leq M(\hat{h}) < 1024$	256
$1024 \leq M(\hat{h}) < 4096$	1024

Since the data rate of M-QAM is $R = \frac{T_d}{T}\log_2(M)$, the following optimization problem is introduced,

$$R = \max_{x_t, P_t, T_t, P_d(\hat{h})} \frac{T_d}{T} E\left[\log_2\left(1 + K\frac{P_d(\hat{h})\hat{h}^2}{P_d(\hat{h})\sigma_{\tilde{h}}^2 + 1}\right)\right] \quad \textbf{(3.28)}$$

where the expectation is with respect to the channel estimate. In order to simplify the analysis it is assumed in (Soysal, Ulukus & Clancy 2008) that the power allocation is constant, $P_d(\hat{h}) = P_d$. Consequently, the scheme in (Soysal, Ulukus & Clancy 2008) is adaptive in constellation size but not adaptive in power. However, this constant power allocation scheme results in very low data rates for low to moderate SNR values. In particular, data rate is almost zero when SNR is 0 dB.

The optimization problem in (3.28) is over the training symbol x_t, training phase duration T_t, training power P_t, and data transmission power $P_d(\hat{h})$, where $E[P_d(\hat{h})]T_d + P_tT_d = PT$ due to conservation of energy. Since the transmitter does not know the channel before the training phase, training symbol, power, and duration cannot depend on the estimated channel. Therefore, the methods from (Hassibi & Hochwald 2003) can be applied here. First, $\hat{h} = \sigma_{\hat{h}}\bar{h}$ is defined so that $\bar{h}$ is unit variance. Now the training symbol, x_t, can be found to be

$$x_t x_t^H = T_t \quad \textbf{(3.29)}$$

by maximizing the effective SNR, $P_{eff} = \frac{P_d \sigma_{\hat{h}}^2}{P_d(\hat{h})\sigma_{\hat{h}}^2+1}$ (Hassibi & Hochwald 2003). Note that, any training signal that has unit-energy is optimum. Next, by following (Hassibi & Hochwald 2003), it is easy to show that the rate is an increasing function of T_d, and hence a decreasing function of T_t. Setting T_t to its minimum value is optimum, which in our case is $T_t = 1$. This might seem counter-intuitive at first. However, a longer training phase implies a shorter data transmission phase, as the block length (coherence time) is fixed. A shorter data transmission phase, in turn, implies a smaller achievable rate. Since data transmission length appears as a linear coefficient to the rate and the training length appears inside the logarithm of the achievable rate, using the minimum possible training length makes sense while maximizing the achievable rate. Finally, dividing the total power into training power and data power can be done by following (Hassibi & Hochwald 2003). Since the total energy is conserved, we have

$$PT = P_t T_t + P_d T_d \quad \textbf{(3.30)}$$

Let α denote the fraction of energy that is devoted to the data transmission,

$$P_d T_d = \alpha PT \qquad P_t T_t = (1-\alpha)PT, 0 < \alpha < 1 \quad \textbf{(3.31)}$$

the fraction of energy that is devoted to the data transmission can be found by following (Soysal, Ulukus & Clancy 2008)

$$\alpha = \begin{cases} \frac{1}{2} & T_d = 1 \\ \gamma - \sqrt{\gamma(\gamma - 1)} & T_d > 1 \end{cases} \quad \textbf{(3.32)}$$

where $\gamma = \frac{1+PT}{PT\left(1-\frac{1}{T_d}\right)}$.

From (Hassibi & Hochwald 2003), the variance of channel estimation error $\sigma_{\tilde{h}}^2$ and the variance of estimated channel $\sigma_{\hat{h}}^2$ are

$$\sigma_{\hat{h}}^2 = \frac{P_t x_t^H x_t}{1+P_t x_t^H x_t} \qquad \sigma_{\tilde{h}}^2 = \frac{1}{1+P_t x_t^H x_t} \quad \textbf{(3.33)}$$

In the next section, power adaptation is considered as well as constellation size adaptation in order to increase the achievable data transmission rate at low SNR regime.

3.3 POWER ALLOCATION SCHEMES

After optimizing the training parameters in the previous section, the optimization problem reduces to

$$R = \max_{E[P_d(\hat{h})]<P_d} \frac{T_d}{T} E\left[\log_2\left(1 + K\frac{P_d(\hat{h})\hat{h}^2}{P_d(\hat{h})\sigma_{\tilde{h}}^2 + 1}\right)\right] \quad \textbf{(3.34)}$$

Although (3.34) is not necessarily a convex problem, KKT condition will still give us a local maximum. Therefore, in order to derive a power allocation scheme, we will use the following Lagrangian of (3.34),

$$\frac{T_d}{T}E\left[\log_2\left(1+K\frac{P_d(\hat{h})\hat{h}^2}{P_d(\hat{h})\sigma_{\tilde{h}}^2+1}\right)\right]-\lambda(E[P_d(\hat{h})-P_d) \quad \textbf{(3.35)}$$

where λ is the Lagrange multiplier. KKT condition is found by taking the derivative of (3.35) with respect to $P_d(\hat{h})$,

$$\frac{T_d}{T}\left(\frac{\sigma_{\tilde{h}}^2+K\hat{h}^2}{P_d(\hat{h})(\sigma_{\tilde{h}}^2+K\hat{h}^2)+1}-\frac{\sigma_{\tilde{h}}^2}{P_d(\hat{h})\sigma_{\tilde{h}}^2+1}\right)-\lambda\leq 0 \quad \textbf{(3.36)}$$

KKT condition is satisfied with equality, when $P_d(\hat{h})$ is non-zero. In order to pull $P_d(\hat{h})$ from (3.36) we re-arrange the terms in (3.36) to get the following quadratic equation

$$\sigma_{\tilde{h}}^2(\sigma_{\tilde{h}}^2+K\hat{h}^2)P_d^2(\hat{h})+(2\sigma_{\tilde{h}}^2+K\hat{h}^2)P_d(\hat{h})+\left(1-\frac{K\hat{h}^2}{\frac{\lambda T}{T_d}}\right)=0 \quad \textbf{(3.37)}$$

The solution to the above quadratic equation can be found as,

$$P_d(\hat{h})=\frac{-(2\sigma_{\tilde{h}}^2+K\hat{h}^2)\pm\sqrt{\left(K\hat{h}^2\right)^2+\frac{4\sigma_{\tilde{h}}^2K\hat{h}^2(\sigma_{\tilde{h}}^2+K\hat{h}^2)}{\frac{\lambda T}{T_d}\ln 2}}}{2\sigma_{\tilde{h}}^2(\sigma_{\tilde{h}}^2+K\hat{h}^2)} \quad \textbf{(3.38)}$$

After simplifying the previous equation, we have the following power allocation policy $P_d(\hat{h})$,

$$P_d(\hat{h}) = \left(-\frac{1}{2\left(\sigma_{\tilde{h}}^2 + K\hat{h}^2\right)} - \frac{1}{2\sigma_{\tilde{h}}^2} + \sqrt{\Delta}\right)^+ \qquad \textbf{(3.39)}$$

Where $\Delta = \frac{K^2\hat{h}^4}{4\left(\sigma_{\tilde{h}}^4\right)\left(\sigma_{\tilde{h}}^2 + K\hat{h}^2\right)^2} + \frac{K\hat{h}^2 T_d}{\lambda T \sigma_{\tilde{h}}^2(\sigma_{\tilde{h}}^2 + K\hat{h}^2)}$. Note that the power allocation policy in (3.39) depends on the inverse of the channel estimation, similar to the water-filling policy that depends on the inverse of actual channel when receiver has the perfect CSI. However it also depends on the BER and training phase duration. Due to the relation of the data rate to (3.26), allocating power using (3.39) always satisfies the BER condition. Since the power allocation policy in (3.39) is a little complicated than the classical water-filling solution, we propose another scheme based on water-filling idea. Water-filling is the optimum power allocation that results in the highest possible data rate when the receiver has perfect CSI. In such a case, optimum power allocation policy is obtained in (Goldsmith & Chua 1997) as,

$$P_d(h) = \left(\frac{1}{\grave{\lambda}} - \frac{1}{h^2}\right)^+ \qquad \textbf{(3.40)}$$

where $\grave{\lambda}$ is the Lagrange multiplier for the capacity maximization problem, and it is different than λ of our problem. It is important to note that in (3.40), $\boldsymbol{h}$ is the actual channel and both the receiver and transmitter know the channel perfectly and instantaneously. However, in our model the channel is estimated, and both the receiver and transmitter have only access to the estimated channel, $\hat{\boldsymbol{h}}$. Under this assumption, we propose to use the same form in (3.40), but by replacing the actual channel with the estimated channel. In this case, the power allocation policy becomes

$$P_d(\hat{h}) = \left(\frac{1}{\mu} - \frac{1}{\hat{h}^2}\right)^+ \qquad \textbf{(3.41)}$$

where μ is the constant that satisfies the average power constraint, $E[P_d(\hat{h})] = P_d$. Although this power allocation policy is easier to compute, it does not take the effect of BER into account, and it is likely to result in a higher BER. Therefore when stringent BER restrictions are in effect, it might be better to utilize (3.39).

3.4 NUMERICAL ANALYSIS

In this section, the proposed power allocation schemes are compared to the constant power allocation and we observe that for low to moderate SNR values, the data rate can be tripled. In Figure 3.1, it is observed that achieved data rates using the solution to KKT condition and the water-filling-like scheme are very close to each other, and they are significantly higher than the rate with constant power allocation. The increase in performance is more emphasized for low SNR values which is practically the case in cellular systems. As SNR increases, data rate advantage decreases. Another point is that the solution to KKT condition always result in a better rate, although it is not possible to see the difference in Figure 3.1. In order to observe the difference between proposed schemes, the realized BER performances are plotted in Figure 3.2. It is important to note that, as a result of our development, realized BER has to stay below the target BER when constant power allocation and the power allocation in (3.39) are used. However, water-filling-like power allocation scheme does not consider the effect of BER, and realized BER in this case might result in a higher value than the target BER. When the target BER is 10^{-3}, we see that at especially low SNR values, realized BER from water-filling-like power allocation scheme exceeds the target BER. This validates our previous comment that utilizing the power allocation strategy in (3.39) is better under stringent BER constraints. In Figure 3.3, we plot allocated power values with respect to the absolute value of the estimated channel. We observe that the power allocation in (3.39) puts more power to better channels than the water-filling-like scheme does, while allocated powers to worse channels are almost the same. As a result of allocating more power to better channels, smaller number of errors occur. Figure 3.4 and Figure 3.5 show the achieved data rate and BER realization when target BER$= 10^{-2}$, respectively.

Figure 3.1: Comparison of achievable data rates when target BER=10^{-3}

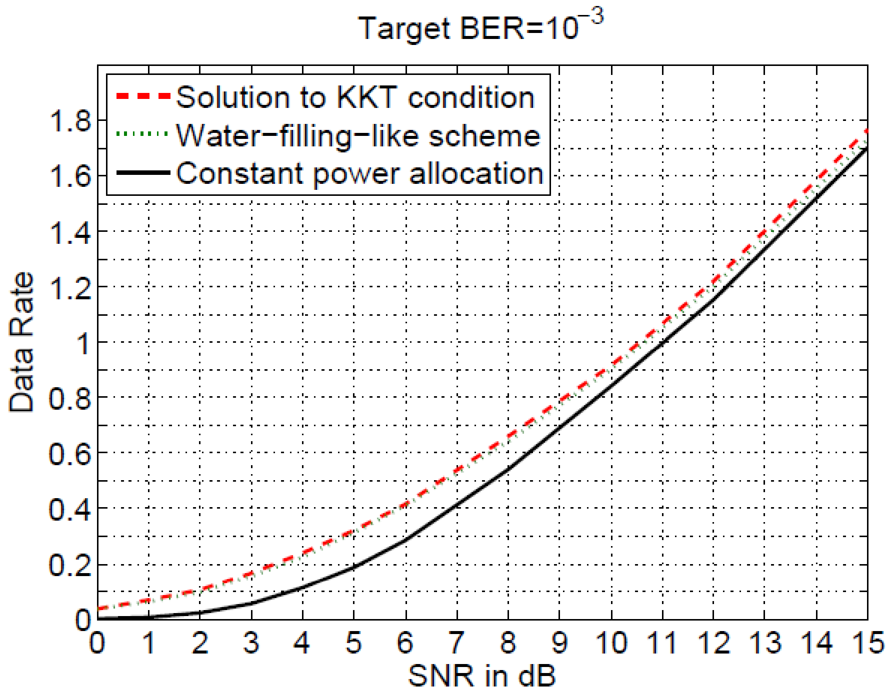

Figure 3.2: Realized BER for a fixed target BER=10^{-3}.

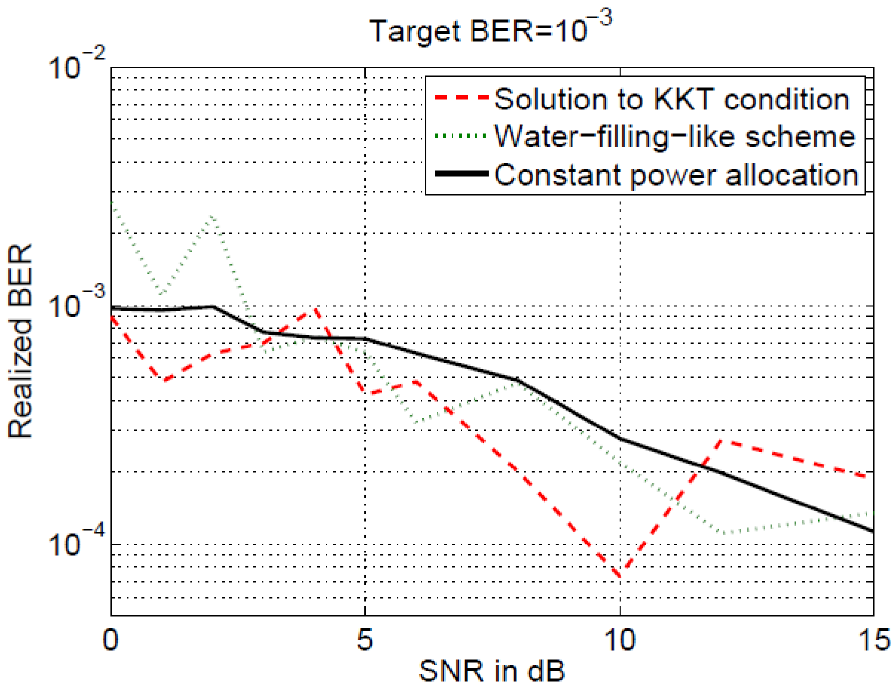

Figure 3.3: Allocated power values over the absolute value of the estimated channel where BER=10^{-3} and average power P=1 for all three schemes.

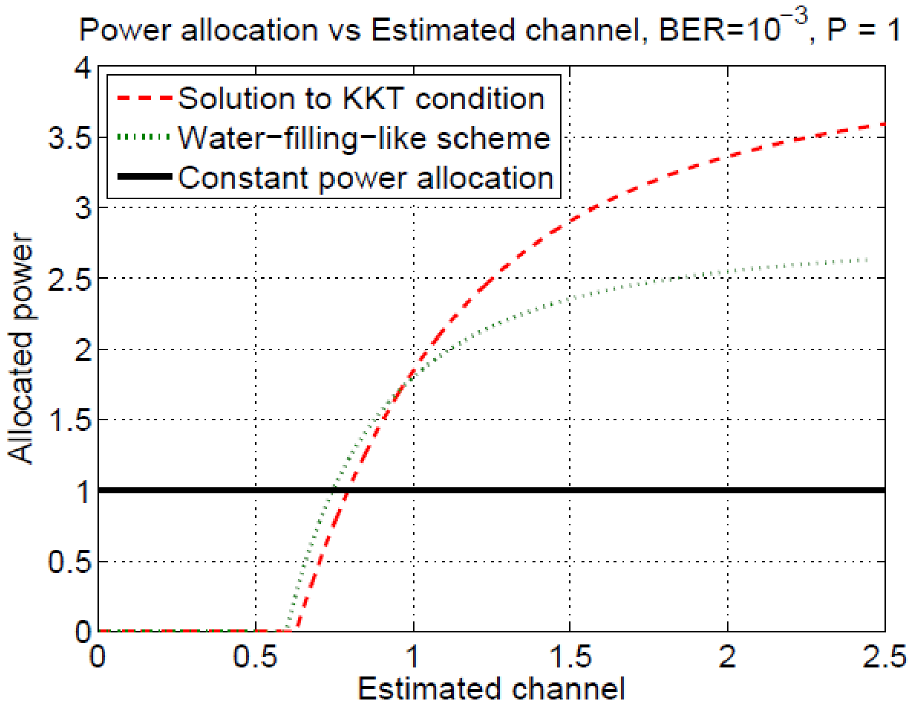

Figure 3.4: Comparison of achievable data rates when target BER=10^{-2}

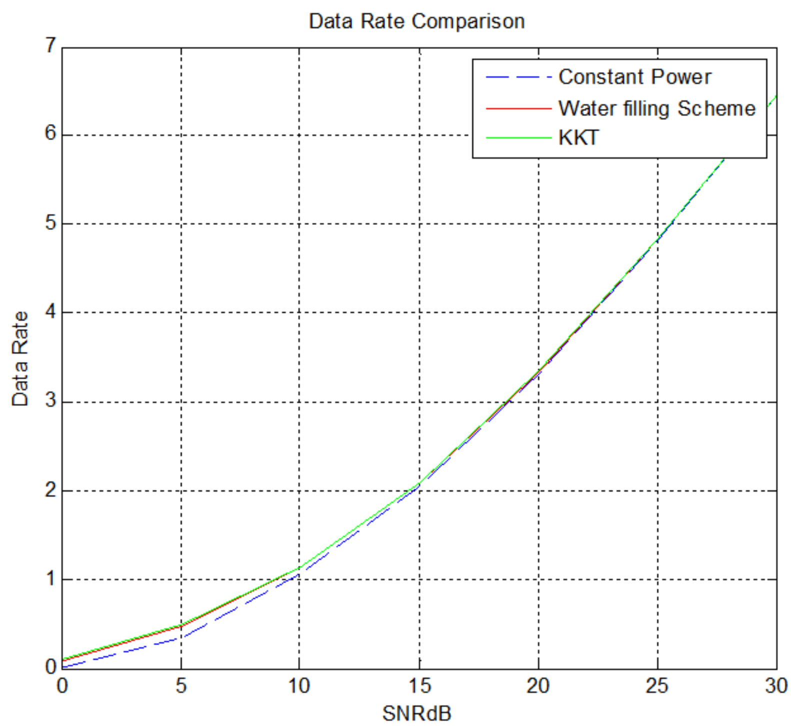

Figure 3.5: Realized BER for a fixed target BER=10^{-2}

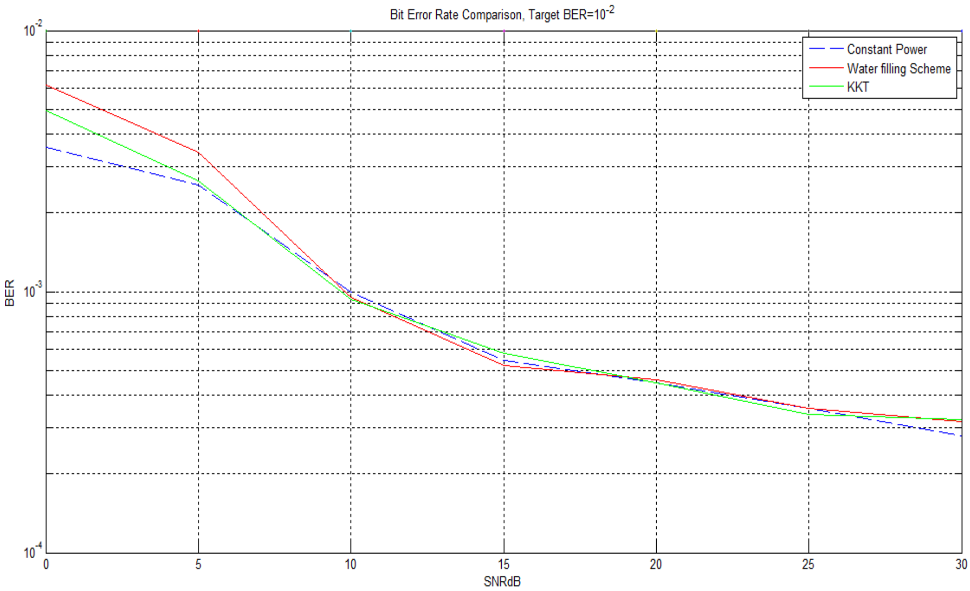

4. ADAPTIVE MODULATION IN MULTIPLE ANTENNA SYSTEMS

Multiple Input Multiple Output (MIMO) technology has seen considerable attention over the last decade because of its ability to increase the data rate and decrease BER without increasing bandwidth or transmitted power. In this chapter, adaptive modulation with multiple antennas is proposed. Channel estimation error is considered in designing the system, and successive decoding technique is applied in the receiver side.

4.1 MULTIPLE INPUT MULTIPLE OUTPUT (MIMO)

Due to high demand of data rate in the wireless communication systems, several types of diversity techniques have been used to increase the spectral efficiency and provide high system performance. Diversity types can be classified into three types: *time diversity*, *frequency diversity* and *spatial diversity*. In time diversity, different time slots and channel coding can be used. While in frequency diversity, the signal is transmitted using several frequencies such as in orthogonal frequency division multiplexing (OFDM). However, in spatial diversity the signal is transmitted over multiple propagation paths. Spatial diversity can be achieved by using multiple antennas in the transmit or/and receiver sides. In general, multiple antenna systems are known as multiple input multiple output (MIMO) systems. In the last decade, MIMO systems have emerged as the most promising technology in increasing data rate and decreasing bit error rate (BER) of wireless transmission systems (PAULRAJ et al. 2004). In (Telatar 1999) it has been approved that MIMO technique increases the capacity with no cost of extra spectrum.

A MIMO system consists of N_t transmit and N_r receive antennas as it is illustrated in Figure 4.1. In receiver side, each antenna receives the direct component intended for it and the indirect components intended from other antennas. Mathematically, MIMO transmission can be shown as the following

$$\boldsymbol{Y} = \boldsymbol{H}\boldsymbol{X} + \boldsymbol{N} \tag{4.1}$$

where $\mathbf{Y}$ is $N_r \times T$ output vector, $\boldsymbol{X}$ is $N_t \times T$ input vector, $\boldsymbol{N}$ is $N_r \times T$ noise vector and $\boldsymbol{H}$ is $N_r \times N_t$ channel matrix.

Figure 4.1: MIMO Scheme

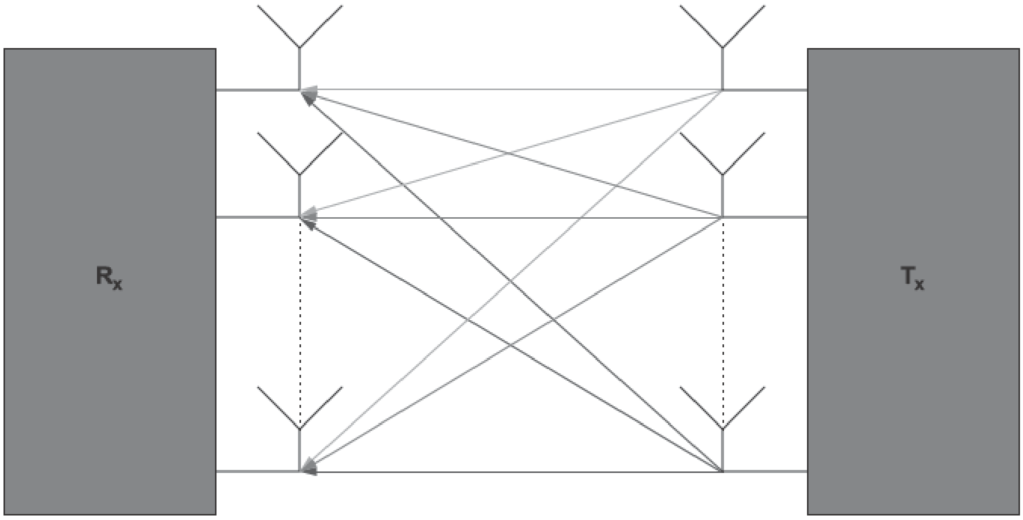

Source: Sibille, Oestges & Zanella 2010

With respect to the number of users, MIMO system can be classified to: Single User SU-MIMO and Multi User MU-MIMO. In SU-MIMO system, data stream is divided into the number of antennas and this leads to increase in the data rate. While, in MU-MIMO, individual data streams are transmitted through transmit antennas as it is shown in Figure 4.2. MU-MIMO is useful uplink transmissions in Long Term Evolution (LTE).

There are different techniques in MIMO systems to improve wireless system performance. Three types of MIMO techniques are explained: *Spatial Diversity*, *Spatial Multiplexing*, and *Beamforming*.

In Beamforming (Sesia, Toufik & Baker 2009), same signal is transmitted through different antennas with different phases. While in spatial diversity (PAULRAJ et al. 2004), increasing transmission performance is the main purpose. There are two types of spatial diversity, namely *Receiver diversity* and *Transmitter diversity*. In receiver diversity, more antenna on the receiver side are used.

Figure 4.2: Multi user MU-MIMO

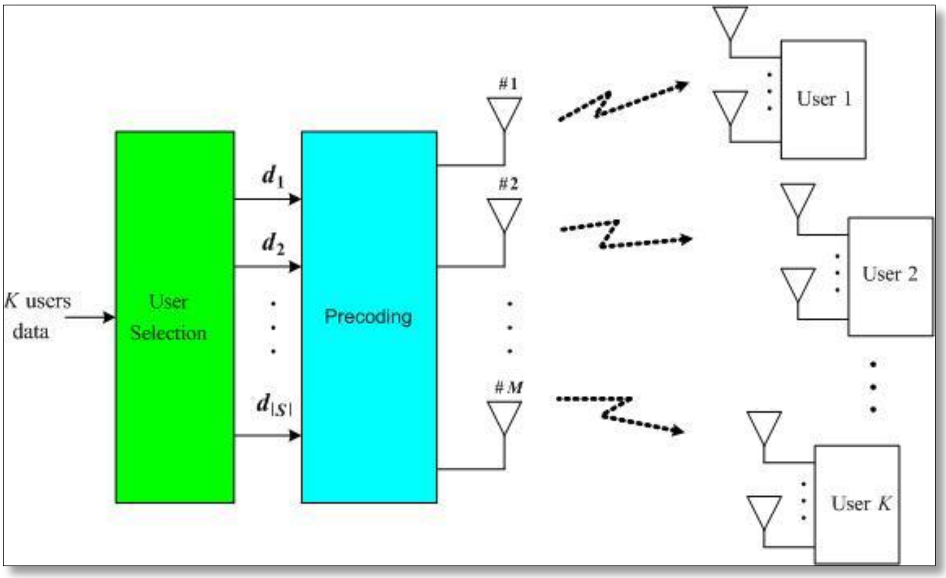

The simplest form of receiver diversity is Single Input Multiple Output (SIMO) where one antenna is used in the transmitter side and two antennas in the receiver side. In transmitter diversity, more antennas are used on the transmitter side and the simplest form is Multiple Input Single Output (MISO) as it is shown in Figure 4.3. Implementing transmitter diversity can be done by using space time codes and the first code for two antennas was developed by Alamouti (Alamouti 1998). While in spatial multiplexing, data is divided into separate streams, these streams are transmitted independently by separate antennas as it is show in Figure 4.4.

4.1.1 Applications of MIMO

MIMO scheme has been implemented in many telecommunication technologies such as wireless Local Area Network (LAN), Mesh Networks, and WiMAX 802.16e. MIMO is also combined with Orthogonal Frequency Division Multiplexing (OFDM) to be the main core of Long Term Evolution (LTE) technology

Figure 4.3: Multiple Antennas forms.

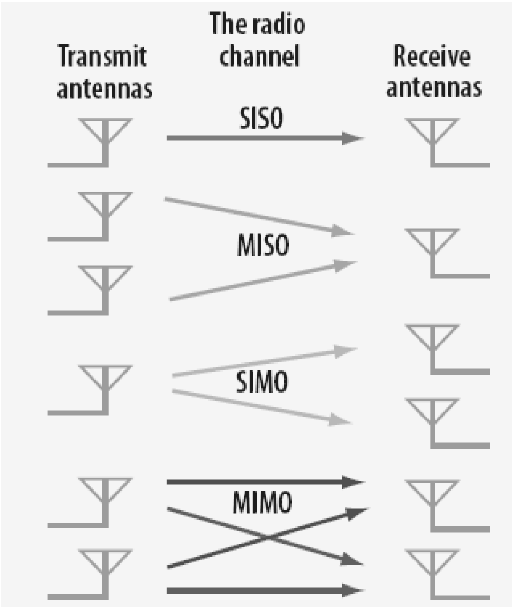

Source: Rumney & Whitacre 2008

Figure 4.4: Spatial Multiplexing MIMO Transmitter

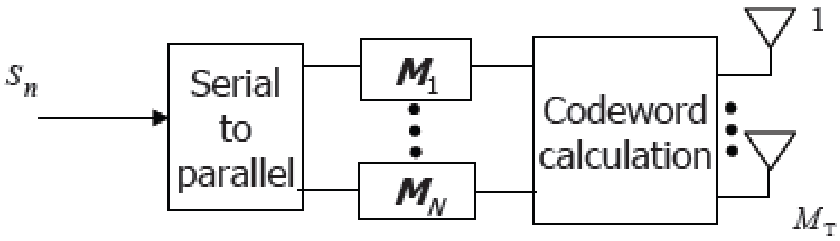

4.2 SUCCESSIVE DECODING

Successive decoding technique (also called Successive Interference Cancellation) improves the performance of MIMO transmission systems by detecting the interference and cancelling the projected effect of the interference on the data in a serial fashion. In the receiver side of a MIMO system, each antenna receives the direct component from the opposite antenna in the transmitter and receives the indirect components from other transmit antennas. These indirect components act as interference in the receiver since the desired signal is the direct component. This problem can be solved by applying decoding process in sequence, after decoding the first symbol in the first antenna, the decoded symbol is eliminated from other antennas. Therefore, this leads to a decrease in the interference gradually, then the last antenna will be clear from the other antenna's interference. Figure 4.5 shows the successive decoding process in MIMO system. Successive decoding is also widely used in MU-MIMO, the receiver decodes the transmitted bits user-by-user. After cancelling the interference from the previously decoded users by using the bits from the previous user and discard it from the current user. Successive decoding improves MIMO system in two ways:

a. It decreases the interference
b. Each successive layer estimated has a higher gain than the previous

However, the main disadvantage in successive decoding is that if an error occurs in decoding the symbol in an antenna then this error will affect the following antennas.

Figure 4.5: Successive Decoding Procedure

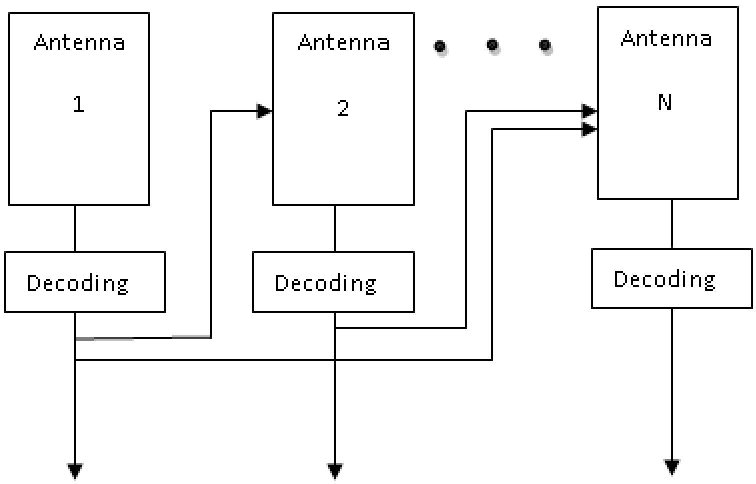

4.3 SYSTEM MODEL

In our model, equal number of transmit and receive antennas are used, $N_T = N_R = 2$, where N_T and N_R are the number of transmit and receive antennas, respectively. Although two antennas is not high, 2×2MIMO is used in current wireless communication systems such as IEEE 802.11n and in LTE systems. The elements of channel matrix $\boldsymbol{H}$ between the transmitter and the receiver are assumed to be a circularly-symmetric complex Gaussian random variables, i.e., Rayleigh fading. As in the previous chapter, a block fading scenario is assumed where the channel stays constant for T symbols and changes to an i.i.d realization during block transitions. The received signal $N_R \times 1$ vector can be represented as

$$\boldsymbol{y}_r = \sqrt{\frac{P}{N_T}}\boldsymbol{H}\boldsymbol{x}_r + \boldsymbol{n}_r \ \ , r = 1,2, \ldots, T \tag{4.2}$$

where $\boldsymbol{n}_r \sim \mathcal{CN}(0, \boldsymbol{I})$ is $N_R \times 1$ noise vector, and the entries of $N_R \times N_T$ $\boldsymbol{H}$ are complex Gaussian random variables. The input signal $N_T \times 1$ $\boldsymbol{x}$ has a unit average power constraint, $E[|\boldsymbol{x}|^2] \leq 1$, P is the average SNR. As in single antenna system, each block is divided into training and data transmission phases, where the training sequence has length T_t, and the data sequence has length $T_d = T - T_t$. In order to demodulate the transmitted symbols, the channel has to be estimated at the receiver side. Channel matrix elements are estimated in the receiver and fed back to the transmitter. Feedback link is assumed to be error free and instantaneous in this analysis.

4.4 CHANNEL ESTIMATION

To assure good quality of channel estimation, known training bits are transmitted during the training phase. Using these training bits, channel matrix elements can be estimated. From (Hassibi & Hochwald 2003), the optimum length of T_t is equal to the number of transmitted antennas which is equal to two in our case, then the input-output relation of the channel during the training phase is

$$\boldsymbol{y}_{\boldsymbol{t}_r} = \sqrt{\frac{P_t}{N_T}}\boldsymbol{H}\boldsymbol{x}_{\boldsymbol{t}_r} + \boldsymbol{n}_{\boldsymbol{t}_r} \ \ , r = 1,2, \ldots, T_t \tag{4.3}$$

where P_t is the SNR of the training symbol, $\boldsymbol{y_t}$, $\boldsymbol{x_t}$ and $\boldsymbol{n_t}$ represent the received signal, the transmitted signal and the noise vectors, respectively. The power constraint for the $N_t \times T_t$ training input signal matrix $\boldsymbol{X_t}$ is $\frac{1}{T_t} tr(\boldsymbol{X}_t^H \boldsymbol{X}_t) \leq N_t$. In our case, $T_t = N_t = 2$ and channel matrix $\boldsymbol{H}$ is

$$H = \begin{bmatrix} h_{11} & h_{12} \\ h_{21} & h_{22} \end{bmatrix} \quad \textbf{(4.4)}$$

Then, the received signal vector can be written in single variable form as,

$$\begin{aligned} \mathbf{y_{1_t}} &= \sqrt{\frac{\mathrm{P_t}}{2}} \mathrm{h}_{11} \mathbf{x_{1_t}} + \sqrt{\frac{\mathrm{P_t}}{2}} \mathrm{h}_{12} \mathbf{x_{2_t}} + \mathbf{n_{1_t}} \\ \mathbf{y_{2_t}} &= \sqrt{\frac{\mathrm{P_t}}{2}} \mathrm{h}_{21} \mathbf{x_{1_t}} + \sqrt{\frac{\mathrm{P_t}}{2}} \mathrm{h}_{22} \mathbf{x_{2_t}} + \mathbf{n_{2_t}} \end{aligned} \quad \textbf{(4.5)}$$

where the length of $\boldsymbol{y}_t, \boldsymbol{x}_t$ is $1 \times T_t$. Then , four equations are existed as the following

$$\begin{aligned} \mathrm{y_{1_t}}(1) &= \sqrt{\frac{\mathrm{P_t}}{2}} \mathrm{h}_{11} \mathrm{x_{1_t}}(1) + \sqrt{\frac{\mathrm{P_t}}{2}} \mathrm{h}_{12} \mathrm{x_{2_t}}(1) + \mathrm{n_{1_t}}(1) \\ \mathrm{y_{1_t}}(2) &= \sqrt{\frac{\mathrm{P_t}}{2}} \mathrm{h}_{11} \mathrm{x_{1_t}}(2) + \sqrt{\frac{\mathrm{P_t}}{2}} \mathrm{h}_{12} \mathrm{x_{2_t}}(2) + \mathrm{n_{1_t}}(2) \\ \mathrm{y_{2_t}}(1) &= \sqrt{\frac{\mathrm{P_t}}{2}} \mathrm{h}_{21} \mathrm{x_{1_t}}(1) + \sqrt{\frac{\mathrm{P_t}}{2}} \mathrm{h}_{22} \mathrm{x_{2_t}}(1) + \mathrm{n_{2_t}}(1) \\ \mathrm{y_{2_t}}(2) &= \sqrt{\frac{\mathrm{P_t}}{2}} \mathrm{h}_{21} \mathrm{x_{1_t}}(2) + \sqrt{\frac{\mathrm{P_t}}{2}} \mathrm{h}_{22} \mathrm{x_{2_t}}(2) + \mathrm{n_{2_t}}(2) \end{aligned} \quad \textbf{(4.6)}$$

where the number between the brackets is the value of T_t. From (Hassibi & Hochwald 2003), the optimum $N_t \times T_t$ training signal matrix $\boldsymbol{X}_t$ satisfies

$$\boldsymbol{X}\boldsymbol{X}^{\boldsymbol{H}} = \begin{bmatrix} N_t & \cdots & 0 \\ \vdots & \ddots & \vdots \\ 0 & \cdots & N_t \end{bmatrix} \quad \textbf{(4.7)}$$

For 2×2 MIMO, $T_t = N_t = 2$. Therefore signal which satisfies (4.7) is

$$\boldsymbol{X_t} = \begin{bmatrix} 1 & 1 \\ 1 & -1 \end{bmatrix} \quad \textbf{(4.8)}$$

After inserting (4.8) in (4.6), we have the following

$$\begin{aligned} y_{1_t}(1) &= \sqrt{\frac{\mathrm{P_t}}{2}}\mathrm{h}_{11} + \sqrt{\frac{\mathrm{P_t}}{2}}\mathrm{h}_{12} + \mathrm{n}_{1_\mathrm{t}}(1) \\ y_{1_t}(2) &= \sqrt{\frac{\mathrm{P_t}}{2}}\mathrm{h}_{11} - \sqrt{\frac{\mathrm{P_t}}{2}}\mathrm{h}_{12} + \mathrm{n}_{1_\mathrm{t}}(2) \end{aligned} \quad \textbf{(4.9)}$$

and for the second antenna, we have

$$\begin{aligned} y_{2_t}(1) &= \sqrt{\frac{\mathrm{P_t}}{2}}\mathrm{h}_{21} + \sqrt{\frac{\mathrm{P_t}}{2}}\mathrm{h}_{22} + \mathrm{n}_{2_\mathrm{t}}(1) \\ y_{2_t}(2) &= \sqrt{\frac{\mathrm{P_t}}{2}}\mathrm{h}_{21} - \sqrt{\frac{\mathrm{P_t}}{2}}\mathrm{h}_{22} + \mathrm{n}_{2_\mathrm{t}}(2) \end{aligned} \quad \textbf{(4.10)}$$

where $y_{i_t}(1)$ and $y_{i_t}(2)$ are the outputs of the ith antenna at $T_t = 1$ and $T_t = 2$ respectively. Before using channel estimation techniques, the above equations can be simplified by summing $y_{1_t}(1)$ to $y_{1_t}(2)$, then we have

$$y_{1_t}(1) + y_{1_t}(2) = 2\sqrt{\frac{\mathrm{P_t}}{2}}\mathrm{h}_{11} + \mathrm{n}_{1_\mathrm{t}}(1) + \mathrm{n}_{1_\mathrm{t}}(2) \tag{4.11}$$

and similarly for $y_{2_t}(1)$ and $y_{2_t}(2)$

$$y_{2_t}(1) + y_{2_t}(2) = 2\sqrt{\frac{\mathrm{P_t}}{2}}\mathrm{h}_{21} + \mathrm{n}_{2_\mathrm{t}}(1) + \mathrm{n}_{2_\mathrm{t}}(2) \tag{4.12}$$

while h_{12} and h_{22} can be found by subtracting $y_{1_t}(1)$ from $y_{1_t}(2)$ and $y_{2_t}(1)$ and $y_{2_t}(2)$ respectively,

$$y_{1_t}(1) - y_{1_t}(2) = 2\sqrt{\frac{\mathrm{P_t}}{2}}\mathrm{h}_{12} + \mathrm{n}_{1_\mathrm{t}}(1) - \mathrm{n}_{1_\mathrm{t}}(2) \tag{4.13}$$

$$y_{2_t}(1) - y_{2_t}(2) = 2\sqrt{\frac{\mathrm{P_t}}{2}}\mathrm{h}_{22} + \mathrm{n}_{2_\mathrm{t}}(1) - \mathrm{n}_{2_\mathrm{t}}(2) \tag{4.14}$$

By using linear MMSE estimation method, the estimated channel elements van be written as

$$\begin{aligned}
\hat{h}_{11} &= C_1{}^H\left(y_{1_t}(1) + y_{1_t}(2)\right)\\
\hat{h}_{12} &= C_2{}^H\left(y_{1_t}(1) - y_{1_t}(2)\right)\\
\hat{h}_{21} &= C_3{}^H\left(y_{2_t}(1) + y_{2_t}(2)\right)\\
\hat{h}_{22} &= C_4{}^H\left(y_{2_t}(1) + y_{2_t}(2)\right)
\end{aligned} \tag{4.15}$$

where $\boldsymbol{C}^H$ is the constant which minimize the channel estimation error. In order to find the optimum linear MMSE estimator, one has to solve the optimization problem with $\hat{h}_{ij}$ and $\tilde{h}_{ij} = h_{ij} - \hat{h}_{ij}$,

$$\min_{c} E\left[\tilde{h}_{ij}\tilde{h}_{ij}{}^{*}\right] = \min_{c} E\left[\left(h_{ij} - \hat{h}_{ij}\right)\left(h_{ij} - \hat{h}_{ij}\right)^{*}\right] \tag{4.16}$$

To solve the above problem, the orthogonality principle is applied. Therefore, the constant $\boldsymbol{C}^H$ which satisfies (4.16) is calculated as the following

$$E\left[\left(h_{11} - \hat{h}_{11}\right)\left(\boldsymbol{y}_{1_t}(1) + \boldsymbol{y}_{1_t}(2)\right)^{*}\right] = 0 \tag{4.17}$$

By inserting $\hat{h}_{11}$ in (4.17), we have

$$E\left[\left(h_{11} - C_1{}^H\left(y_{1_t}(1) + y_{1_t}(2)\right)\right)\left(y_{1_t}(1) + y_{1_t}(2)\right)^{*}\right] = 0 \tag{4.18}$$

By using the linearity property of the expectation, we have

$$C_1{}^H = \frac{E\left[h_{11}\left(y_{1_t}(1) + y_{1_t}(2)\right)^{*}\right]}{E\left[\left(y_{1_t}(1) + y_{1_t}(2)\right)\left(y_{1_t}(1) + y_{1_t}(2)\right)^{*}\right]} \tag{4.19}$$

Since we know that the channel and noise are independent and each of them is zero mean with unity variance, then the constant $\boldsymbol{C}^H$ becomes

$$C_1{}^H = \frac{\sqrt{.5P_t}}{1+P_t} \qquad \textbf{(4.20)}$$

By using the same calculations to find C_2^H, C_3^H, C_4^H, we found that they are equal to (4.20). After estimating the channel, the channel matrix is fed back to the transmitter and transmitter regards it as the actual channel while channel estimation error is added to noise to be the effective noise.

4.5 DATA TRANSMISSION PHASE

In this process we have the following received signal

$$\boldsymbol{y}_{\boldsymbol{d}_r} = \sqrt{\frac{P_d}{N_T}}(\widehat{\boldsymbol{H}} + \widetilde{\boldsymbol{H}})\boldsymbol{x}_{\boldsymbol{d}_r} + \boldsymbol{n}_{\boldsymbol{d}_r} \ , r = 1,2, \dots, T_d \qquad \textbf{(4.21)}$$

And we can write each element of $\boldsymbol{y}_{\boldsymbol{d}_r}$ as

$$\mathbf{y}_{\mathbf{1_d}} = \sqrt{\frac{\mathrm{P_d}}{2}}\hat{\mathrm{h}}_{11}\mathbf{x}_{\mathbf{1_d}} + \sqrt{\frac{\mathrm{P_d}}{2}}\hat{\mathrm{h}}_{12}\mathbf{x}_{\mathbf{2_d}} + \sqrt{\frac{\mathrm{P_d}}{2}}\tilde{\mathrm{h}}_{11}\mathbf{x}_{\mathbf{1_d}} + \sqrt{\frac{\mathrm{P_d}}{2}}\tilde{\mathrm{h}}_{12}\mathbf{x}_{\mathbf{2_d}} + \mathbf{n}_{\mathbf{1_d}} \qquad \textbf{(4.22)}$$

$$\mathbf{y}_{\mathbf{2_d}} = \sqrt{\frac{\mathrm{P_d}}{2}}\hat{\mathrm{h}}_{21}\mathbf{x}_{\mathbf{1_d}} + \sqrt{\frac{\mathrm{P_d}}{2}}\hat{\mathrm{h}}_{22}\mathbf{x}_{\mathbf{2_d}} + \sqrt{\frac{\mathrm{P_d}}{2}}\tilde{\mathrm{h}}_{21}\mathbf{x}_{\mathbf{1_d}} + \sqrt{\frac{\mathrm{P_d}}{2}}\tilde{\mathrm{h}}_{22}\mathbf{x}_{\mathbf{2_d}} + \mathbf{n}_{\mathbf{2_d}} \qquad \textbf{(4.23)}$$

In this section variable rate M-QAM is implemented, square M-QAM is used due to its ease of implementation. Square M-QAM can be considered as a combination of two $\sqrt{M}$-PAM, one as the in phase component and the other as the quadrature component as it is explained in chapter 2.

In single antenna case, by using Maximum Likelihood detection, BER was found in (Soysal, Ulukus & Clancy 2008), however in MIMO systems finding BER is more complex than it is in single antenna case because of multiple channel components $(h_{11}, h_{12}h_{21}\ , h_{22})$.

In MIMO systems, we find BER for each antenna separately by using Successive Decoding technique and by assuming that the effective noise $\tilde{\boldsymbol{n}}_{\mathbf{1}}$ is

$$\tilde{\boldsymbol{n}}_{\mathbf{1}} = \sqrt{\frac{\mathrm{P_d}}{2}}\hat{\mathrm{h}}_{12}\mathbf{x}_{\mathbf{2_d}} + \sqrt{\frac{\mathrm{P_d}}{2}}\tilde{\mathrm{h}}_{11}\mathbf{x}_{\mathbf{1_d}} + \sqrt{\frac{\mathrm{P_d}}{2}}\tilde{\mathrm{h}}_{12}\mathbf{x}_{\mathbf{2_d}} + \mathbf{n}_{\mathbf{1_d}} \qquad \textbf{(4.24)}$$

After decoding $\mathbf{x}_{\mathbf{1_d}}$ with the knowledge of the channel $\hat{\mathrm{h}}_{21}$, the component $\sqrt{\mathrm{P_d}/2}\,\hat{\mathrm{h}}_{21}\mathbf{x}_{\mathbf{1_d}}$ is subtracted from (4.23) then BER of second antenna is calculated as the same as the single antenna case in (Soysal, Ulukus & Clancy 2008).

4.6 Deriving BER

In $\sqrt{M_k}$-PAM scheme where k refers to the antenna, one dimensional signal points has value of $\frac{A_{k_i}}{\sqrt{2}}$, where A_{k_i} is the amplitude of the signal point in k$^{\text{th}}$ antenna, and $\sqrt{2}$ comes from the energy of the carrier signal. The amplitude values can be expressed as $A_{k_i} = \left(2i - 1 - \sqrt{M_k}\right)d_k$, where the Euclidean distance between adjacent signal points is $d\sqrt{2}$. By assuming equally probable signals, the average energy of the in-phase component is

$$\begin{aligned} \frac{P_d\left(\hat{h}\right)T_p}{2} &= \frac{1}{\sqrt{M_k}}\sum_{i=1}^{\sqrt{M_k}}\frac{{A_{k_i}}^2}{2} \\ &= \frac{(M_k - 1)d_k^2}{6} \end{aligned} \qquad \textbf{(4.25)}$$

Without loss of generality, T_p is assumed to be equal to one, then

$$d_k^2 = \frac{3P_d\left(\hat{h}\right)}{M_k - 1} \quad \textbf{(4.26)}$$

where $\frac{P_d(\hat{h})}{2}$ is the power allocated to $\sqrt{M_k}$-PAM component. Since A_i is transmitted as the in-phase component and A_j as the quadrature component of the transmitted signal, after match filtering and low band conversion, the received complex signal is written as

$$\boldsymbol{y_n} = \frac{1}{\sqrt{2}}\boldsymbol{HA_{ij}} + \boldsymbol{n_r} \ \ , r = 1,2, \dots, T \quad \textbf{(4.27)}$$

where $\boldsymbol{A_{ij}}$ is a vector that contains the symbols which are transmitted from both antennas. Each element of this complex vector is $\boldsymbol{A_{k_{ij}}} = \boldsymbol{A_{k_i}} + \boldsymbol{jA_{k_j}}$, and the complex matrix $\boldsymbol{H} = \boldsymbol{H}_x + j\boldsymbol{H}_y$. While the additive noise $\boldsymbol{N}$ is circularly symmetric complex Gaussian with independent real and imaginary parts. Since there is channel estimation, we have $\boldsymbol{H} = \widehat{\boldsymbol{H}} + \widetilde{\boldsymbol{H}}$. Consequently,

$$\boldsymbol{y_r} = \frac{1}{\sqrt{2}}\widehat{\boldsymbol{H}}A_{ij} + \frac{1}{\sqrt{2}}\widetilde{\boldsymbol{H}}A_{ij} + \boldsymbol{n_r} \quad \textbf{(4.28)}$$

4.7 DECISION REGIONS with CHANNEL ESTIMATION ERROR

The calculation of BER for a MIMO system in this thesis consists of two different BER calculations at two antennas. These calculations differ due to the successive cancellation technique.

4.7.1 Decision Regions in The First Antenna

In the first antenna the output signal is

$$\boldsymbol{y_1} = \frac{1}{\sqrt{2}} A_{1_{ij}} \hat{h}_{11} + \underbrace{\frac{1}{\sqrt{2}} A_{2_{ij}} \hat{h}_{12} + \frac{1}{\sqrt{2}} A_{1_{ij}} \tilde{h}_{11} + \frac{1}{\sqrt{2}} A_{2_{ij}} \tilde{h}_{12} + \boldsymbol{n_1}}_{\text{effective noise}} \qquad \textbf{(4.29)}$$

In this case, the receiver in the first antenna regards the channel $\hat{h}_{11}$ as the actual channel and the rest of the terms as additional noise. In order to find the decision regions, maximum likelihood rule is used, which states that the signal point (i, j) is decoded if $f(y|m_x, m_y)$ is maximum for $m_x = i, m_y = j$. For the in-phase component, the decision region corresponding to signal point i can be found as the region satisfying

$$f(\boldsymbol{y_1}|i, j, \hat{h}) \geq f(\boldsymbol{y_1}|i+1, j, \hat{h}) \qquad \textbf{(4.30)}$$

$$f(\boldsymbol{y_1}|i, j, \hat{h}) \geq f(\boldsymbol{y_1}|i-1, j, \hat{h}) \qquad \textbf{(4.31)}$$

Because of imperfection of channel estimation, it is difficult to solve these inequalities analytically. The right and the left side boundaries of the decision region corresponding to i can be found by solving $f(y_1|i, j, \hat{h}) = f(y_1|i+1, j, \hat{h})$ and $f(y_1|i, j, \hat{h}) = f(y_1|i-1, j, \hat{h})$. It is assumed that pdf's that are considered in this analysis only intersects with their neighbors (Soysal, Ulukus & Clancy 2008). Then, the right side boundary of the decision region corresponding to i can be found by solving the following

$$f(y_1|i, j, \hat{h}) = f(y_1|i+1, j, \hat{h}) \qquad \textbf{(4.32)}$$

$$\frac{\exp\left(\frac{-\left(y_1-\frac{A_{1_i}}{\sqrt{2}}\left|\hat{h}_{11}\right|\right)^2}{2\tilde{\sigma}_{1_i}^{\,2}}\right)}{\sqrt{\tilde{\sigma}_{1_i}^{\,2}}}=\frac{\exp\left(\frac{-\left(y_1-\frac{A_{1_i}}{\sqrt{2}}\left|\hat{h}_{11}\right|-\sqrt{2}d_1\left|\hat{h}_{11}\right|\right)^2}{2\tilde{\sigma}_{1_{i+1}}^{\,2}}\right)}{\sqrt{\tilde{\sigma}_{1_{i+1}}^{\,2}}} \qquad \textbf{(4.33)}$$

By taking the natural logarithm of both sides of (4.33), we have

$$\ln\left(\tilde{\sigma}_{1_i}^{\,2}\right)+\frac{z_1^2}{\tilde{\sigma}_{1_i}^{\,2}}=\ln\tilde{\sigma}_{1_{i+1}}^{\,2}+\frac{\left(z_1-\sqrt{2}d_1\left|\hat{h}_{11}\right|\right)^2}{\tilde{\sigma}_{1_{i+1}}^{\,2}} \qquad \textbf{(4.34)}$$

Where $z_1=\tilde{n}_1+\frac{A_{2mx}}{\sqrt{2}}\left|\hat{h}_{12}\right|=y_1-\frac{A_{1mx}}{\sqrt{2}}\left|\hat{h}_{11}\right|$, $\tilde{n}_1=\frac{1}{\sqrt{2}}A_{1_{ij}}\tilde{h}_{11}+\frac{1}{\sqrt{2}}A_{2_{ij}}\tilde{h}_{12}+n_1$, and $\tilde{\sigma}_{1_i}^{\,2}$ is the variance of the in-phase component of effective noise z_1 which can be found by calculating the variance of the effective noise z_1 as the following

$$\tilde{\sigma}_1^2=\tilde{\sigma}_{1_i}^{\,2}+\tilde{\sigma}_{1_j}^{\,2} \qquad \textbf{(4.35)}$$

where $\tilde{\sigma}_{1_j}^{\,2}$ is the variance of the quadrature component of effective noise z_1

By assuming that both variance of in-phase and quadrature component are equal,

$$\begin{aligned}\tilde{\sigma}_{1_i}^{\,2}&=\frac{1}{2}E[z_1z_1^*]\\&=\frac{1}{2}E\left[\frac{1}{2}A_{2_{ij}}\hat{h}_{12}A_{2_{ij}}^*\hat{h}_{12}^*+\frac{1}{2}A_{1_{ij}}\tilde{h}_{11}A_{1_{ij}}^*\tilde{h}_{11}^*+\frac{1}{2}A_{1_{ij}}\tilde{h}_{12}A_{2_{ij}}^*\tilde{h}_{12}^*+n_1n_1^*\right]\end{aligned} \qquad \textbf{(4.36)}$$

By using the linearity of expectation and moving $A_{1_{ij}}$ and $A_{2_{ij}}$ outside of expectation, then

$$\tilde{\sigma}_{1_i}^{\,2} = \frac{1}{2}\left(\frac{1}{2}A_{2_{ij}}^{\,2}\underbrace{E\left[\hat{h}_{12}^{2}\right]}_{\hat{\sigma}_{12}^{2}} + \frac{1}{2}A_{1_{ij}}^{\,2}\underbrace{E\left[\tilde{h}_{11}^{2}\right]}_{\tilde{\sigma}_{11}^{2}} + \frac{1}{2}A_{2_{ij}}^{\,2}\underbrace{E\left[\tilde{h}_{12}^{2}\right]}_{\tilde{\sigma}_{12}^{2}} + \underbrace{E\left[n_1^2\right]}_{1}\right) \qquad \textbf{(4.37)}$$

Since h_{12} has unit variance, then

$$\sigma_{12}^2 = \hat{\sigma}_{12}^2 + \tilde{\sigma}_{12}^2 = 1 \qquad \textbf{(4.38)}$$

Then, the variance of the in-phase component of the effective noise is

$$\tilde{\sigma}_{1_i}^{\,2} = \frac{1}{2}\left[\frac{A_{2_i}^{\,2} + A_{2_j}^{\,2}}{2} + \frac{A_{1_i}^{\,2} + A_{1_j}^{\,2}}{2}\sigma_{\tilde{h}_{11}}^2 + 1\right] \qquad \textbf{(4.39)}$$

The main goal in this calculation is to find $\tilde{n}_1$ expression in the right and left side boundaries. Therefore, after using the value of $z_1 = \tilde{n}_1 + \frac{A_{2mx}}{\sqrt{2}}\left|\hat{h}_{12}\right|$ we have

$$\frac{\left(\tilde{n}_1 + \frac{A_{2_i}}{\sqrt{2}}\left|\hat{h}_{12}\right|\right)^2}{\tilde{\sigma}_{1_i}^{\,2}} = \ln\frac{\tilde{\sigma}_{1_{i+1}}^{\,2}}{\tilde{\sigma}_{1_i}^{\,2}} + \frac{\left(\tilde{n}_1 + \frac{A_{2_i}}{\sqrt{2}}\left|\hat{h}_{12}\right| - \sqrt{2}d_1\left|\hat{h}_{11}\right|\right)^2}{\tilde{\sigma}_{1_{i+1}}^{\,2}} \qquad \textbf{(4.40)}$$

This results in the following equation,

$$\frac{\tilde{n}_1^2 + \frac{\rho^2}{2} + 2\frac{\rho}{\sqrt{2}}\tilde{n}_1}{\tilde{\sigma}_{1_i}^{\,2}} = \ln\frac{\tilde{\sigma}_{1_{i+1}}^{\,2}}{\tilde{\sigma}_{1_i}^{\,2}} + \frac{\tilde{n}_1^2 + \frac{\rho^2}{2} + 2\varphi^2 + \frac{2\rho\tilde{n}_1}{\sqrt{2}} - 2\sqrt{2}\varphi\tilde{n}_1 - 2\varphi\rho}{\tilde{\sigma}_{1_{i+1}}^{\,2}} \qquad \textbf{(4.41)}$$

where $\rho = A_{2_i}\left|\hat{h}_{12}\right|$ and $\varphi = d_1\left|\hat{h}_{11}\right|$. From (Soysal, Ulukus & Clancy 2008), it is assumed that non-canceling terms containing square of $\tilde{n}_1$ are small enough. When the terms which include $\tilde{n}_1$ are moved to the left part, we have

$$\frac{2\frac{\rho}{\sqrt{2}}\tilde{n}_1}{\tilde{\sigma}_{1_i}^{\ 2}} - \frac{2\frac{\rho\tilde{n}_1}{\sqrt{2}} + 2\sqrt{2}\varphi\tilde{n}_1}{\tilde{\sigma}_{1_{i+1}}^{\ 2}} = \ln\frac{\tilde{\sigma}_{1_{i+1}}^{\ 2}}{\tilde{\sigma}_{1_i}^{\ 2}} + \frac{\frac{\rho^2}{2}}{\tilde{\sigma}_{1_i}^{\ 2}} + \frac{\frac{\rho^2}{2} + 2\varphi^2 - 2\varphi\rho}{\tilde{\sigma}_{1_{i+1}}^{\ 2}} \tag{4.42}$$

By unifying the denominator of (4.42) and taking $\tilde{n}_1$ as a common factor in the left side of (4.42) we have

$$\tilde{n}_1\left(\frac{\frac{2\rho}{\sqrt{2}}\tilde{\sigma}_{1_{i+1}}^{\ 2} - \left(\frac{2\rho}{\sqrt{2}} + 2\sqrt{2}\varphi\right)\tilde{\sigma}_{1_i}^{\ 2}}{\tilde{\sigma}_{1_i}^{\ 2}\tilde{\sigma}_{1_{i+1}}^{\ 2}}\right) = \frac{\emptyset + \frac{\rho^2}{2}\tilde{\sigma}_{1_i}^{\ 2} + \left(\frac{\rho^2}{2} + 2\varphi^2 - 2\varphi\rho\right)\tilde{\sigma}_{1_{i+1}}^{\ 2}}{\tilde{\sigma}_{1_{i+1}}^{\ 2}\tilde{\sigma}_{1_i}^{\ 2}} \tag{4.43}$$

Where $\emptyset = \tilde{\sigma}_{1_{i+1}}^{\ 2}\tilde{\sigma}_{1_i}^{\ 2}\ln\frac{\tilde{\sigma}_{1_{i+1}}^{\ 2}}{\tilde{\sigma}_{1_i}^{\ 2}}$, then $\tilde{n}_1$becomes

$$\tilde{n}_1 = \frac{\tilde{\sigma}_{1_i}^{\ 2}\tilde{\sigma}_{1_{i+1}}^{\ 2}\ln\frac{\tilde{\sigma}_{1_{i+1}}^{\ 2}}{\tilde{\sigma}_{1_i}^{\ 2}} - \frac{\rho^2}{2}\tilde{\sigma}_{1_{i+1}}^{\ 2} + \frac{\rho^2}{2}\tilde{\sigma}_{1_i}^{\ 2} + 2\varphi^2\tilde{\sigma}_{1_i}^{\ 2} - 2\varphi\rho\tilde{\sigma}_{1_i}^{\ 2}}{\frac{2\rho}{\sqrt{2}}\tilde{\sigma}_{1_{i+1}}^{\ 2} - \frac{2\rho}{\sqrt{2}}\tilde{\sigma}_{1_i}^{\ 2} + 2\sqrt{2}\varphi\tilde{\sigma}_{1_i}^{\ 2}} \tag{4.44}$$

$$\triangleq \bar{r}_{i|j}$$

In a similar way, the left side boundary of the decision region corresponding to i can be found by solving

$$\frac{\exp\left(\frac{-\left(y_1-\frac{A_{1_i}}{\sqrt{2}}\left|\hat{h}_{11}\right|\right)^2}{2\tilde{\sigma}_{1_i}^{\;2}}\right)}{\sqrt{\tilde{\sigma}_{1_i}^{\;2}}}=\frac{\exp\left(\frac{-\left(y_1-\frac{A_{1_i}}{\sqrt{2}}\left|\hat{h}_{11}\right|+\sqrt{2}d_1\left|\hat{h}_{11}\right|\right)^2}{2\tilde{\sigma}_{1_{i-1}}^{\;2}}\right)}{\sqrt{\tilde{\sigma}_{1_{i-1}}^{\;2}}} \tag{4.45}$$

By taking the natural logarithm of both sides of (4.45)

$$\frac{z_1^2}{\tilde{\sigma}_{1_i}^{\;2}}=\ln\frac{\tilde{\sigma}_{1_{i-1}}^{\;2}}{\tilde{\sigma}_{1_i}^{\;2}}+\frac{\left(z_1+\sqrt{2}d_1\left|\hat{h}_{11}\right|\right)^2}{\tilde{\sigma}_{1_{i-1}}^{\;2}} \tag{4.46}$$

This results in the following equation,

$$\frac{\left(\tilde{n}_1+\frac{A_{2_i}}{\sqrt{2}}\left|\hat{h}_{12}\right|\right)^2}{\tilde{\sigma}_{1_i}^{\;2}}=\ln\frac{\tilde{\sigma}_{1_{i-1}}^{\;2}}{\tilde{\sigma}_{1_i}^{\;2}}+\frac{\left(\tilde{n}_1+\frac{A_{2_i}}{\sqrt{2}}\left|\hat{h}_{12}\right|+\sqrt{2}d_1\left|\hat{h}_{11}\right|\right)^2}{\tilde{\sigma}_{1_{i-1}}^{\;2}} \tag{4.47}$$

By using similar calculations as in the case of right side boundary, we have the following

$$\frac{\tilde{n}_1^2+\frac{\rho^2}{2}+2\frac{\rho}{\sqrt{2}}\tilde{n}_1}{\tilde{\sigma}_{1_i}^{\;2}}=\ln\frac{\tilde{\sigma}_{1_{i+1}}^{\;2}}{\tilde{\sigma}_{1_i}^{\;2}}+\frac{\tilde{n}_1^2+\frac{\rho^2}{2}+2\varphi^2+\frac{2\rho\tilde{n}_1}{\sqrt{2}}+2\sqrt{2}\varphi\tilde{n}_1+2\varphi\rho}{\tilde{\sigma}_{1_{i+1}}^{\;2}} \tag{4.48}$$

By removing the square terms of $\tilde{n}_1$, $\tilde{n}_1$ becomes

$$\begin{aligned}\tilde{n}_1&=\frac{\tilde{\sigma}_{1_i}^{\;2}\tilde{\sigma}_{1_{i-1}}^{\;2}\ln\frac{\tilde{\sigma}_{1_{i-1}}^{\;2}}{\tilde{\sigma}_{1_i}^{\;2}}-\frac{\rho^2}{2}\tilde{\sigma}_{1_{i-1}}^{\;2}+\frac{\rho^2}{2}\tilde{\sigma}_{1_i}^{\;2}+2\varphi^2\tilde{\sigma}_{1_i}^{\;2}+2\varphi\rho\tilde{\sigma}_{1_i}^{\;2}}{\frac{2\rho}{\sqrt{2}}\tilde{\sigma}_{1_{i-1}}^{\;2}-\frac{2\rho}{\sqrt{2}}\tilde{\sigma}_{1_i}^{\;2}+2\sqrt{2}\varphi\tilde{\sigma}_{1_i}^{\;2}}\\&\triangleq\bar{l}_{i|j}\end{aligned} \tag{4.49}$$

After combining both edges, the decision region corresponding to i is

$$\bar{l}_{i|j} \leq \tilde{n}_1 \leq \bar{r}_{i|j} \tag{4.50}$$

Now, the in-phase probability of error is written as the probability that the real part of the effective noise is in this region given that (i, j) is transmitted

$$P_{1_{i|j}} = \Pr\left(\bar{l}_{i|j} \leq \tilde{n}_1 \leq \bar{r}_{i|j} | \hat{h}, i, j\right) \tag{4.51}$$

$$= Q\left(\frac{\bar{l}_{i|j}}{\tilde{\sigma}_{1_i}}\right) + Q\left(\frac{\bar{r}_{i|j}}{\tilde{\sigma}_{1_i}}\right) \tag{4.52}$$

By assuming that the right-side boundary for i is the same as the left-side boundary for $i + 1$, then we have the following

$$\sum_i P_{1_{i|j}} = \sum_i 2Q\left(\sqrt{\frac{\bar{r}_{i|j}^2}{\tilde{\sigma}_{1_i}^{\ 2}}}\right) \tag{4.53}$$

$$= \sum_i 2Q\left(\sqrt{\frac{\left(\frac{\tilde{\sigma}_{1_i}^{\ 2}\tilde{\sigma}_{1_{i+1}}^{\ 2}\ln\frac{\tilde{\sigma}_{1_{i+1}}^{\ 2}}{\tilde{\sigma}_{1_i}^{\ 2}} + \frac{\rho^2}{2}\left(\tilde{\sigma}_{1_i}^{\ 2} - \tilde{\sigma}_{1_{i+1}}^{\ 2}\right) + 2\tilde{\sigma}_{1_i}^{\ 2}\varphi(\varphi - \rho)}{2\sqrt{2}\varphi\tilde{\sigma}_{1_i}^{\ 2} - 2\frac{2\rho}{\sqrt{2}}\left(\tilde{\sigma}_{1_i}^{\ 2} - \tilde{\sigma}_{1_{i+1}}^{\ 2}\right)}\right)^2}{\tilde{\sigma}_{1_i}^{\ 2}}}\right) \tag{4.54}$$

For simplicity let's define the new symbols

$$\alpha = \tilde{\sigma}_{1_i}^{\ 2}\, \tilde{\sigma}_{1_{i+1}}^{\ 2} \ln \frac{\tilde{\sigma}_{1_{i+1}}^{\ 2}}{\tilde{\sigma}_{1_i}^{\ 2}}$$
$$\beta = \tilde{\sigma}_{1_i}^{\ 2} - \tilde{\sigma}_{1_{i+1}}^{\ 2} \tag{4.55}$$

Then we have,

$$\sum_i P_{1_{i|j}} = \sum_i 2Q\left(\sqrt{\frac{\left(\dfrac{\alpha + \dfrac{\rho^2}{2}\beta + 2\tilde{\sigma}_{1_i}^{\ 2}\varphi(\varphi-\rho)}{2\sqrt{2}\varphi\tilde{\sigma}_{1_i}^{\ 2} - 2\dfrac{2\rho}{\sqrt{2}}\beta}\right)^2}{\tilde{\sigma}_{1_i}^{\ 2}}}\right) \tag{4.56}$$

$$\sum_i P_{1_{i|j}} = \sum_i 2Q\left(\sqrt{\frac{\nabla + 2\tilde{\sigma}_{1_i}^{\ 2}\varphi(\varphi-\rho)\left(\alpha + \rho^2\beta + 2\tilde{\sigma}_{1_i}^{\ 2}\varphi(\varphi-\rho)\right)}{\tilde{\sigma}_{1_i}^{\ 2}\left(8\varphi^2\tilde{\sigma}_{1_i}^{\ 4} - 8\varphi\tilde{\sigma}_{1_i}^{\ 2}\beta\rho + 8\rho^2\beta^2\right)}}\right) \tag{4.57}$$

where $\nabla = \rho^2\alpha\beta + \frac{\rho^4\beta^2}{4} + \alpha^2$. To find the average probability of error of the in-phase component, averaging the above inequality over i is implemented. An approximate upper bound is obtained by moving both of the averaging summations inside the Q-function. As a result, the terms which contain α and β inside the Q-function turn out to be zero, and we have

$$P_{1_{in}} \lesssim 2Q\left(\sqrt{\frac{d_1^2\left|\hat{h}_{11}\right|^2 + A_{2_i}^{\ 2}\left|\hat{h}_{12}\right|^2}{2\tilde{\sigma}_{1_i}^{\ 2}}}\right) \tag{4.58}$$

By inserting (4.26) in (4.58), we have the following

$$P_{1_{in}} \lesssim 2Q\left(\frac{\frac{3P_{1_d}(\hat{h})}{M_1-1}\left|\hat{h}_{11}\right|^2 + P_{2_d}(\hat{h})\left|\hat{h}_{12}\right|^2}{P_{2_d}(\hat{h}) + P_{1_d}(\hat{h})\sigma^2_{\tilde{h}_{11}} + 1}\right) \quad \textbf{(4.59)}$$

Where $\frac{{A_1}_i^2+{A_1}_j^2}{2} = P_{1_d}(\hat{h})$, and $\frac{{A_2}_i^2+{A_2}_j^2}{2} = P_{2_d}(\hat{h})$

To reduce the complexity, power is assumed to be constant. Therefore, adaptive modulation in this chapter is variable rate constant power and $P_{1_d} = P_{2_d} = \frac{P_d}{2}$. By approximating the Q-function by $Q(x) \approx \frac{1}{2}\exp(-x^2)$, we have

$$P_{1_{in}} \lesssim \exp\left(-\frac{\frac{3P_d}{2(M_1-1)}\left|\hat{h}_{11}\right|^2 + \frac{P_d}{2}\left|\hat{h}_{12}\right|^2}{\frac{P_d}{2} + \frac{P_d}{2}\sigma^2_{\tilde{h}_{11}} + 1}\right) \quad \textbf{(4.60)}$$

The BER of M-QAM over the in-phase and quadrature components becomes

$$BER_1(\hat{h}) \leq P_{in} + P_q \quad \textbf{(4.61)}$$

$$\lesssim 2\exp\left(-\frac{\frac{3P_d}{2(M_1-1)}\left|\hat{h}_{11}\right|^2 + \frac{P_d}{2}\left|\hat{h}_{12}\right|^2}{\frac{P_d}{2} + \frac{P_d}{2}\sigma^2_{\tilde{h}_{11}} + 1}\right) \quad \textbf{(4.62)}$$

The previous equation says that when M-QAM is used with estimated channels $\hat{h}_{11}, \hat{h}_{12}$ then the resulting BER is less than the right hand side of (4.62). When choosing the size of constellation, we can set the target BER to the right hand side of (4.62), this results in

BER for the transmission less that the target BER. Then maximum constellation size for a given BER is

$$M_1(\hat{h}) = 1 + \frac{-3|\hat{h}_{11}|^2}{|\hat{h}_{12}|^2 + \ln(.5BER)\left(1 + \sigma_{\tilde{h}_{11}}^2 + \frac{2}{P_d}\right)} \quad \textbf{(4.63)}$$

4.7.2 Decision Regions in The Second Antenna

In the second antenna, we have

$$y_2 = \frac{1}{\sqrt{2}}A_{1_{ij}}\hat{h}_{21} + \frac{1}{\sqrt{2}}A_{2_{ij}}\hat{h}_{22} + \frac{1}{\sqrt{2}}A_{1_{ij}}\tilde{h}_{21} + \frac{1}{\sqrt{2}}A_{2_{ij}}\tilde{h}_{22} + n_2 \quad \textbf{(4.64)}$$

After detecting the first symbol A_1in the first antenna and with knowledge of $\hat{h}_{21}$, $\frac{1}{\sqrt{2}}A_{1_{ij}}\hat{h}_{21}$ can be cancelled from (4.64). Consequently, effective noise becomes

$$\tilde{n}_2 = \frac{1}{\sqrt{2}}A_{1_{ij}}\tilde{h}_{21} + \frac{1}{\sqrt{2}}A_{2_{ij}}\tilde{h}_{22} + n_2 \quad \textbf{(4.65)}$$

Since the effective noise is decreased, data rate is increased too. By utilizing maximum likelihood rule, BER expression is derived and is the same as in (Soysal, Ulukus & Clancy 2008) which is explained in the previous chapter.

However, in our case the variance of the in-phase component of the effective noise in the second antenna $\tilde{\sigma}_{2_i}^{\,2}$ is derived as the following

$$\tilde{\sigma}_{2_i}^{\,2} = \frac{1}{2}E[\tilde{n}_2\tilde{n}_2^*] \quad \textbf{(4.66)}$$

$$= \frac{1}{2} E\left[\frac{1}{2} A_{1_{ij}} \widetilde{h}_{21} A_{1_{ij}}^{*} \widetilde{h}_{21}^{*} + \frac{1}{2} A_{2_{ij}} \widetilde{h}_{22} A_{2_{ij}}^{*} \widetilde{h}_{22}^{*} + n_2 n_2^{*}\right]$$

$$\tilde{\sigma}_{2_i}^{\,2} = \frac{1}{2}\left(\frac{A_{2_i}^{\,2} + A_{2_i}^{\,2}}{2}\sigma_{\widetilde{h}_{22}}^{2} + \frac{A_{1_i}^{\,2} + A_{1_i}^{\,2}}{2}\sigma_{\widetilde{h}_{21}}^{2} + 1\right) \quad \textbf{(4.67)}$$

As the previous chapter in single antenna case, we follow (Soysal, Ulukus & Clancy 2008) and probability of error becomes

$$P_{2_{in}} \lesssim \exp\left(-\frac{\frac{3P_d}{2(M_2-1)}\left|\hat{h}_{22}\right|^2}{\frac{P_d}{2}\sigma_{\widetilde{h}_{21}}^{2} + \frac{P_d}{2}\sigma_{\widetilde{h}_{22}}^{2} + 1}\right) \quad \textbf{(4.68)}$$

Finally, the BER of M-QAM over the in-phase and quadrature components in the second antenna becomes

$$BER_2(\hat{h}) \leq P_{2_{in}} + P_{2_q} \quad \textbf{(4.69)}$$

Then, the resulting BER is

$$BER_2(\hat{h}) \lesssim 2\exp\left(\frac{-3\left|\hat{h}_{22}\right|^2}{(M_2-1)\left(\sigma_{\widetilde{h}_{21}}^{2} + \sigma_{\widetilde{h}_{22}}^{2} + \frac{2}{P_d}\right)}\right) \quad \textbf{(4.70)}$$

Therefore, finding the constellation size for the second antenna can be done by equating the target BER to the right hand side of (4.70). Then after arranging (4.70), the maximum constellation size is

$$M_2(\hat{h}) = 1 + \frac{-3|\hat{h}_{22}|^2}{\ln(.5BER)\left(\sigma^2_{\tilde{h}_{21}} + \sigma^2_{\tilde{h}_{22}} + \frac{2}{P_d}\right)} \tag{4.71}$$

The above equation is maximized by minimizing channel estimation error variances. Since $\sigma^2_{\tilde{h}} + \sigma^2_{\hat{h}} = 1$, and we know the estimated channel, the channel estimation error which minimizes (4.71**)** can be find as the following

$$\begin{aligned}\sigma^2_{\tilde{h}} &= 1 - E[\hat{h}\hat{h}^*] \\ &= \frac{1}{1 + P_t x_t^H x_t}\end{aligned} \tag{4.72}$$

After finding constellation size then the data rate of the system is

$$R = \frac{T_d}{T}(\log_2 M_1 + \log_2 M_2) \tag{4.73}$$

4.8 OPTIMAL POWER DISTRIBUTION

Since our scheme is training based, total power is divided into: *training power* and *data power*. Since the total energy is conserved, we have $PT = P_t T_t + P_d T_d$. Let α denotes the fraction of energy that is devoted to the data transmission (Hassibi & Hochwald 2003)

$$P_d T_d = \alpha PT, \qquad P_t T_t = (1-\alpha)PT, \qquad 0 < \alpha < 1 \tag{4.74}$$

The optimum value of α has been shown in (Hassibi & Hochwald 2003) and it is equal to

$$\alpha = \begin{cases} \gamma - \sqrt{\gamma(\gamma-1)} & for\ T_d > N_t \\ \frac{1}{2} & for\ T_d = N_t \\ \gamma - \sqrt{\gamma(\gamma-1)} & for\ T_d > N_t \end{cases} \quad \textbf{(4.75)}$$

where $\gamma = \frac{N_t + PT}{PT\left(1 - \frac{N_t}{T_d}\right)}$.

In our calculations we set the length of the coherence time to be equal four (T=4). Since the optimum length of the training phase T_t equals the number of transmit antennas N_t, then $T_d = T - T_t = 2$ which is equal to the number of transmit antennas too. Therefore, $\alpha = \frac{1}{2}$ and power allocation becomes (Hassibi & Hochwald 2003)

$$P_d = \frac{T}{2N_t}P \qquad P_t = \frac{T}{2(T - N_t)}P \quad \textbf{(4.76)}$$

4.9 NUMERICAL RESULTS

In this section, we use the derived theoretical formulae and computer simulation to evaluate the data rate and BER of the system. We evaluate the performance of the system over channel variations modeled by Rayleigh fading. The new upper bound for BER in first and second antenna are simulated by using Matlab. The data rate for both antennas is plotted. In the simulations, we noticed that the data rate for the new system with MIMO scheme is less than the first antenna and the reason comes from the interference in the first antenna, and half of the power is wasted in the first antenna with high interference. However, by keeping everything same as the single antenna with doubling the power and divide it into both antennas, data rate increased. In Figure 4.6 data rate of adaptive modulation with dividing the power into both antennas is plotted. BER of MIMO system is shown in Figure 4.7, as it is shown values of realized BER are under target BER 10^{-2}. To see the effect of MIMO in increasing the data rate, total power is doubled and each antenna is given the same power. Figure 4.8 and Figure 4.9, show the data rate and BER of Adaptive MIMO, respectively. Data rate is increased and realized BER values are under the target BER.

Figure 4.6: Data rate of adaptive 2×2MIMO system with power dividing

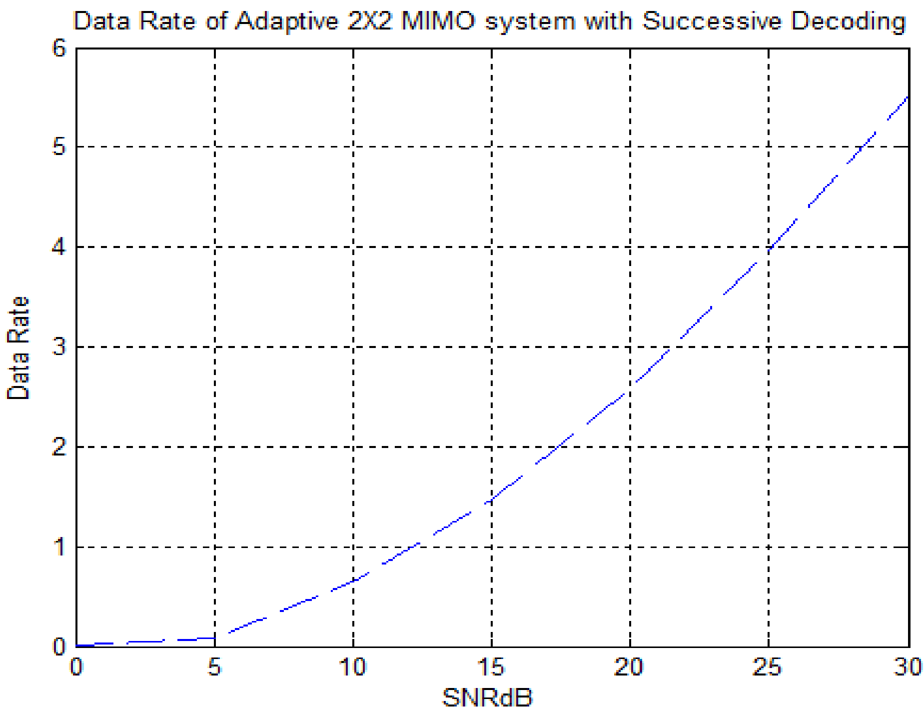

Figure 4.7: BER of Adaptive Modulation with target BER=10^{-2} power dividing

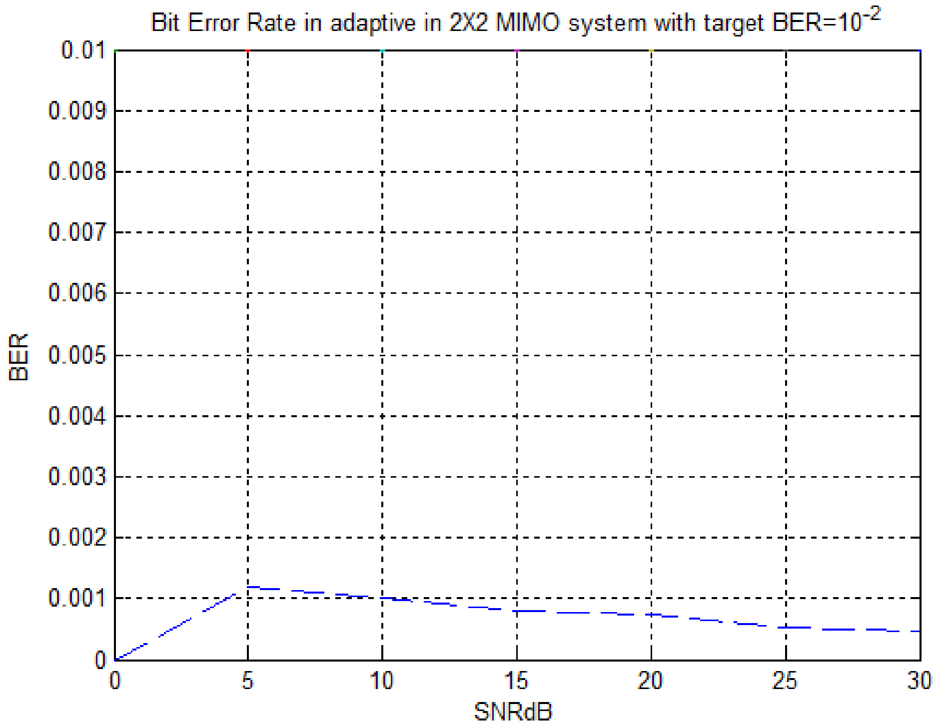

.

Figure 4.8: Data rate of adaptive MIMO system with doubling the total power

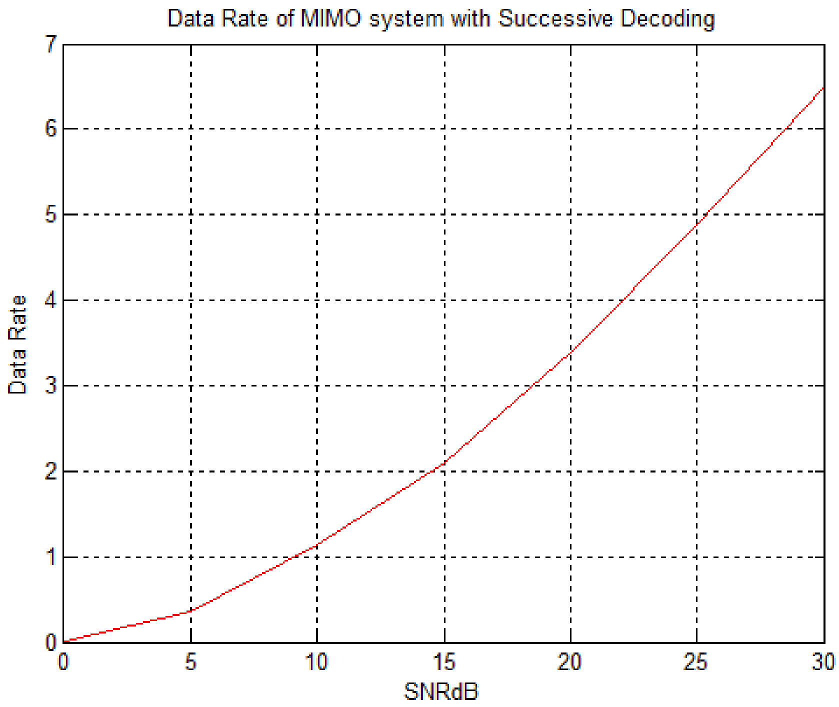

Figure 4.9: BER of Adaptive MIMO system with doubling the total power

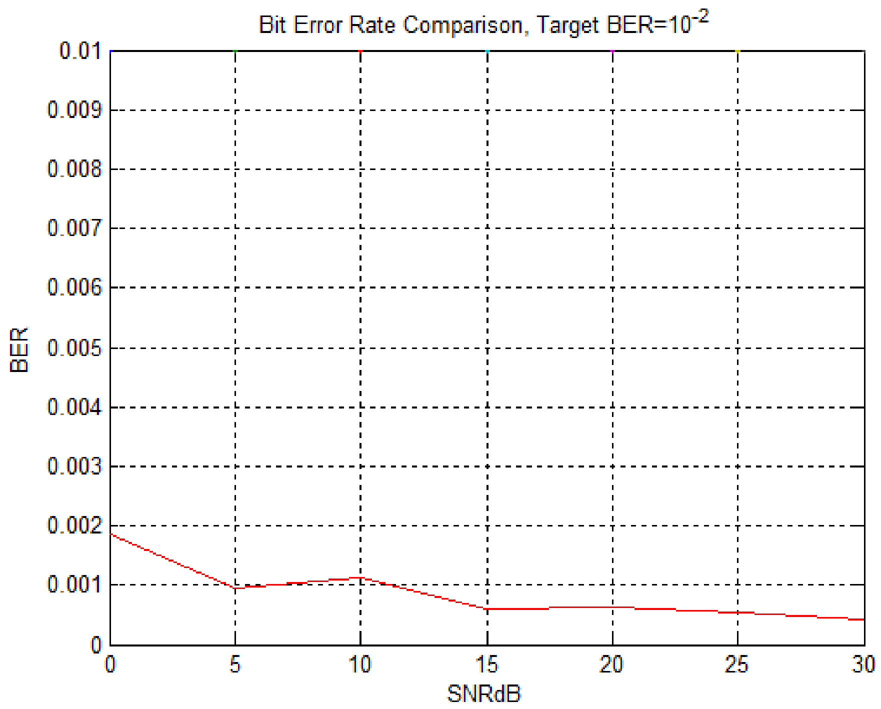

5. CONCLUSIONS

In this thesis, we considered Adaptive modulation. The receiver estimates the channel with possible errors, and the transmitter adapts its power and modulation scheme as a function of the fed-back channel that is estimated at the receiver. It has been shown that in addition to adapting the constellation size of the system, utilizing adaptive power allocation further increases the data rate. At low to moderate SNR values, where modern wireless communications systems operate, the increase in data rate is more pronounced which is up to three times. We also observed that using a simple water-filling-like power allocation scheme can perform as good as the solution to the KKT condition. However, it might violate the BER constraint for stringent target BER values. Furthermore, adaptive modulation in 2×2 MIMO system has been implemented. BER expression for each antenna have been derived. Successive decoding techniques was applied in finding decision regions. We find that data rate is not improved in MIMO because of high interference in the first antenna. Since power allocation is constant half of the power wasted in the first antenna.

Future research plan is to find the power allocation which maximize the spectral efficiency of adaptive MIMO system. Furthermore, extending the number of antennas more than two antennas is our goal in the future.

REFERENCES

Books

Gallager, R. G., 1968. *Information Theory and Reliable Communication*. New York: Wiley.

Goldsmith, A., 2005. *Wireless Communication*. Cambridge University Press.

Haykin, S. 1994. *Communication Systems*. Wiley.

Kamen, E. W. and Su, J. K., 1999. *Introduction to Optimal Estimators*. Springer.

Mcdermott, T., 1998. *Wireless Digital Communications: Design and Theory*. Tucson Amateur Packet Radio Corporation.

Proakis, J. G., 2000. *Digital Communication*. Mc Graw Hill.

Rappaport, T. S., 2002. *Wireless Communications: Principles and Practice*. Prentice Hall.

Sibille, A., Oestges, C., and Zanella, A., 2010. *MIMO: From Theory To Implementation*. Academic Press.

Simon, M. K. and Alouini, M., 2005. *Digital Communication Over Fading Channels*. Wiley.

Sesia, S., Issam, T., and Matthew, B. 2009. *LTE – The Umts Long Term Evolution From Theory To Practice*. Wiley.

Periodicals

Alamouti, S. M. 1998. A Simple Transmit Diversity Technique for Wireless Communications. *IEEE Journal on Select Areas in Communications*. **16**(8), pp. 1451-1458.

Duel-Hallen, A., Hu, S. and Hallen, H., 2000. Long-Range Prediction of Fading: Enabling Adaptive Transmission for Mobile Radio Channels Signals. *IEEE Signal Processing Magazine*. **17**(3), pp. 62- 75.

Chaitanya, B., Sai Ram Prasad, T., Sruthi, K., and Tejaswi, T., 2010. Adaptive Modulation Techniques for Wimax. *International Journal of Computer and Network Security*. **2**(5), pp. 58-61.

Bourles, M., and El Gamal, H., 2004. On The Design of Adaptive Space-Time Codes. *IEEE Transactions on Communications*. **52**(10), pp. 1670- 1674.

Caver, J. K., 1972. Variable-Rate Transmission for Rayleigh Fading Channel. *IEEE Transactions on Communications*. **20**(1), pp. 15-22.

Chung, S. T., and Goldsmith, A., 2001. Degrees Of Freedom In Adaptive Modulation: A Unified View. *IEEE Transactions On Communications*. **49**(9), pp. 1561-1571.

Czylwik, A., 1996. Adaptive Ofdm for Wideband Radio Channels. *Global Telecommunications Conference, 1996.*. London , UK , pp. 713 - 718.

Fernandez-Plazaola, U., Martos-Naya, E., Paris, J. F., and Goldsmith, A., 2010. Adaptive Modulation for Mimo Systems with Channel Prediction Errors. *IEEE Transactions on Wireless Communications*. **9**(8), pp. 2516-2527.

Goeckel, D. L., 1999. Adaptive Coding for Time-Varying Channels Using Outdated Fading Estimates. *IEEE Transactions On Communications*. **47**(6), pp. 844-5-855.

Goldsmith, A., 1998. Adaptive Coded Modulation for Fading Channels. *IEEE Transactions on Communications*. **46**(5), pp. 559-602.

Goldsmith, A., and Soon-Ghee, C., 1997. Variable-Rate Variable-Power MQAM for Fading Channels. *IEEE Transactions on Communications*. **4**(10), pp. 1218 - 1230.

Hassibi, B., and Hochwald, B. M., 2003. How Much Training is Needed in Multiple-Antenna Wireless Links? *IEEE Transactions On Information Theory*. **49**(4), pp. 951 - 963.

Hayes, J. F., 1968. Adaptive Feedback Communications. *IEEE Transactions on Communication Technology*., pp. 29-34.

Ashraful Islam, M., Mondal, R., and Zahid Hasan, M., 2009. Performance Evaluation of Wimax Physical Layer Under Adaptive Modulation Techniques and Communication Channels. *International Journal of Computer Science and Information Security*. **5**(1), pp. 111-114.

Pons, J., and Dunlup, J., 1998. Bit Error Rate Based Link Adaptation for Gsm. *The Ninth IEEE International Symposium on Personal, Indoor and Mobile Radio Communications*.

Torrance, J., and Hanzo, L., 1996. Optimisation Of Switching Levels for Adaptive Modulation in a Slow Rayleigh Fading Channel. *Electronics Letters*. **32**(13), pp. 1167-1169.

Kohno, R., Imai, H., Hatori, M., and Pasupathy, S., 1990. Combination of an Adaptive Array Antenna and a Canceller of Interference for Direct-Sequence Spread-Spectrum Multiple-Access System. *IEEE Journal on Selected Areas in Communications*. **8**(4), pp. 675-682.

Lau, V., and Macleod, M. D., 1997. Variable Rate Adaptive Trellis Coded QAM for High Bandwidth Efficiency Applications in Rayleigh Fading Channels. *Proceedings of The 48th IEEE Vehicular Technology Conference*. Ottawa, pp. 348-352

Li, T., and Collins, O. M., 2007. A Successive Decoding Strategy for Channels with Memory. *IEEE Transactions on Information Theory*. **53**(2), pp. 628-646.

Marzetta, T.L., 1999. Blast Training: Estimating Channel Characteristics for High Capacity Space-Time Wireless. *In Proc. 37th Annual Allerton Conference on Communication, Control, and Computing*.

Mizuno, M., Moriyama, E., Saito, Y., Et Al., 1998. High Speed Multimedia-Multimode Tdma Radio Transmission System for Imt-2000. *Ieice Transactions on Communications*. **E81-B**(7), pp. 1327-1329.

Nakamura, Michiharu, Yassin Awad, And Sunil Vadgama. 2002. Adaptive Control of Link Adaptation for High Speed Downlink Packet Access (HSDPA) n W-CDMA. *The 5th International Symposium on Wireless Personal Multimedia Communications, 2002.*, pp. 382-386.

Narendran, B., Sienicki, J., Yajnik, S., and Agrawal, P., 1997. Evaluation of Adaptive Power and Error Control Algorithm for Wireless Systems. *Icc'97*., pp. 349-355.

Ozdemir, M. and Arslan, H., 2007. Channel Estimation for Wireless OFDM System. *IEEE Communications Surveys*. **9**(2), pp. 19-48.

Paulraj, A. J., Gore, D. A., Nabar, R. U., and Bölcskei, H., 2004. An Overview of MIMO Communications—A Key to Gigabit Wireless. *Proceedings Of The Ieee*. **92**(2), pp. 198-218.

Sadjadpour, H. R., Sloane, N. J. A., Salehi, M., and Nebe, G., 2001. Interleaver Design for Turbo Codes. *IEEE Journal on Selected Areas in Communications*. **19**(5), pp. 831-837.

Shen, Y., and Martinez, E., 2006. Channel Estimation in OFDM Systems. *Freescale Semiconductor*. **1**.

Soysal, Alkan, Ulukus, S., and Clancy, C., 2008. Channel Estimation and Adaptive M-QAM in Cognitive Radio Links. *IEEE International Conference on Communications*. Beijing, China.

Tang, X, Alouini, M., and Goldsmith, A., 1999. Effect of Channel Estimation Error on M-QAM BER Performance in Rayleigh Fading. *IEEE Transactions on Communications*. **47**(12), pp. 1856-1864.

Telatar, I.E. 1999., Capacity of Multiple Antenna Gaussian Channels. *Europ. Trans. Telecomm*. **10**, pp. 585-595.

Torabi, M., and Soleymani, M., 2003. Adaptive Bit Allocation for Space-Time Block Coded OFDM System. *IEEE International Conference on Acoustics, Speech, and Signal Processing, 2003.*

Torrence, J.M., and Hanzo, L., 1996. Upper Bound Performance of Adaptive Modulation in a Slow Rayleigh Fading Channel. *IEEE Electronics Letters*. **32**(8), pp. 718-719.

Ue, T., Sampei, S., and Morinaga, N., 1996. Symbol Rate and Modulation Level Controlled Adaptive Modulation System with TDMA/TDD for High Bit Rate Transmission in High Delay Spread Environments. *Electronics Letters*. **32**(4), pp. 304-305.

Varanasi, M., and Guess, T., 1997. Optimum Decision Feedback Multiuser Equalization with Successive Decoding Achieves The Total Capacity of The Gaussian Multiple-Access Channel. *The Thirty-First Asilomar Conference on Signals, Systems & Computers*., pp. 1405-1409.

Vucetic, B., 1991. An Adaptive Coding Scheme for Time-Varying Channels. *IEEE Transactions on Communications*. **39**(5), pp. 653-663.

Zhendong Z., Vucetic, B., Dohler, M., and Li, Y.H., 2005. Mimo Systems with Adaptive Modulation. *IEEE Transactions on Vehicular Technology*. **54**(5), pp. 1828-1842.

Webb, W. and Steele, R., 1995. Variable Rate Qam for Mobile Radio. *IEEE Transactions on Communications*. **43**, pp. 2223-2230.

Xia, B. and Wang, J., 2005. Effect of Channel-Estimation Error on QAM Systems with Antenna Diversity. *IEEE Transactions on Communications*. **53**(3), pp. 481-488.

Other Sources:

HAAS, I. E., 2004. *Communications Systems* [online]. German Aerospace Center, http://www.kn-s.dlr.de/people/haas/ [Accessed 27 October 2004]

Intersymbol interference (ISI) and Raised Cosine Filtering. [online]. Intuitive Guide to Principles of Communications, http://www.complextoreal.com [Accessed 12 January 2002]

Rumney, M., and Whitacre, J., 2008. *Analyze Antenna Approaches for LTE Wireless Systems*. Microwave and RF, http://www.mwrf.com/Article/ArticleID/19534/19534.html [Accessed 15 August 2008]

CURRICULUM VITAE

Full Name	Mustafa Al-Naqeeb
Address	Talatpaşa cd N.21 Gültepe kağıthane / Istanbul-Turkey mustafa.alnaqeeb@gmail.com
Birth Place/ Date	Baghdad -Iraq/ 12-04-1986
Languages	Arabic (Native), English (Fluent), Turkish (Intermediate)
High School	Jameel Shakir Secondary School
B. Sc	Electronics and Communications Engineering, Alahlyia Amman University 2008
M. Sc	Electrical & Electronics Engineering, Bahçeşehir University, 2011
Name Of Institute	Natural And Applied Sciences
Name Of Program	Electrical and Electronics Engineering

Work Experience :

Mar 2011-Oct 2011

Noya Intenational, Istanbul, Full time Transmission Engineer

June 2008-Oct 2008

Modern Tobacco Company, Amman, Full time Electrical Engineer